ChemComm

Chemical Communications

Accepted Manuscript

This article can be cited before page numbers have been issued, to do this please use: T. Haino, N. Hisano and T. Hirao, *Chem. Commun.*, 2026, DOI: 10.1039/D6CC02170K.

ROYAL SOCIETY OF CHEMISTRY

rsc.li/chemcomm

ChemComm

View Article Online
DOI: 10.1039/D6CC02170K

Feature Article

Supramolecular Polymers Based on Molecular Recognition of Bisporphyrin Clefts

Received 00th January 20xx,
Accepted 00th January 20xx

DOI: 10.1039/x0xx00000x

Takeharu Haino*[a,b], Naoyuki Hisano[a] and Takehiro Hirao[a]

This review highlights supramolecular polymers based on bisporphyrin clefts, which are rigidly linked porphyrin dimers that function as electron-rich molecular tweezers and incorporate three addressable recognition modes: donor–acceptor host–guest complexation, self-complementary dimerization, and metal coordination. These interactions can induce supramolecular polymerization and enable interchange among supramolecular polymer-chain structures, affording attractive functions in solution and in the bulk. This feature article first discusses head-to-tail host–guest complexation–directed step-growth polymerization and ring–chain equilibria of heterotopic monomers bearing both a cleft and an electron-deficient guest, as well as redox regulation of supramolecular polymer chains through redox-tuning of donor–acceptor host–guest complexation. It also describes polymerization driven by self-complementary dimerization, post-polymerization main-chain editing via recognition-pair exchange, and helicity control using built-in or external chirality, affording amplified chiroptical readouts of solvent chirality. Finally, cooperative coupling of host–guest interactions and coordination cross-linking is highlighted as a pathway from supramolecular polymer chains to supramolecular polymer networks, yielding gels and robust free-standing films.

1. Introduction

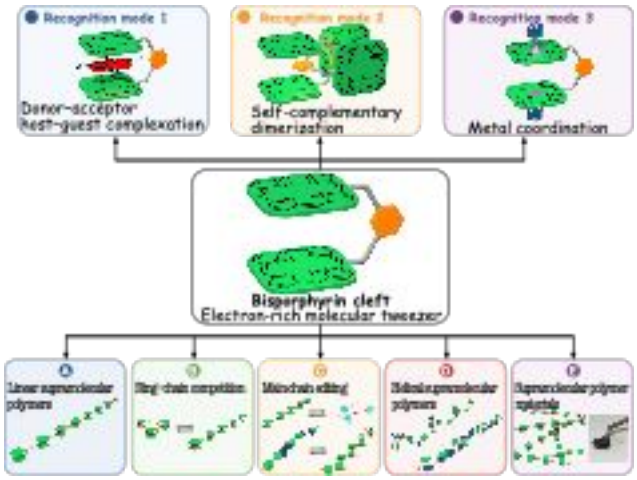

Fig. 1 Roadmap of this review. Bisporphyrin clefts combine donor–acceptor host–guest complexation, self-complementary dimerization, and metal coordination to build and control supramolecular polymers, enabling ring–chain equilibria, redox-responsive chain-length modulation, main-chain editing, helicity control, chiral sensing, and formation of coordination-crosslinked gels and films.

This review conceptualizes bisporphyrin clefts as preorganized molecular tweezers that translate porphyrin-based electronic and chiroptical functions into programmable supramolecular polymerization. Figure 1 provides a roadmap linking each recognition mode to the chain structures, dynamic functions, and materials discussed below.

1.1. Brief background of supramolecular polymers

Supramolecular polymers are chain-like assemblies composed of repeating monomer units interconnected through reversible molecular recognition at complementary binding sites.[1-3] The shift from static covalent bonding to dynamic association in repeating monomer arrays represents a fundamental transformation in the design and development of polymer materials. In supramolecular polymer chains, monomer units recognize one another through noncovalent interactions, including π–π stacking, hydrogen bonding, metal–ligand coordination, and ionic and hydrophobic interactions.[4] Multiple hydrogen bonds provide particularly high specificity in intermolecular association;[5-7] accordingly, they are often employed in supramolecular polymer chemistry.[8-12] Host–guest complexation by macrocyclic hosts such as crown ethers,[13-15] cyclodextrins,[16-18] cucurbiturils,[19-20] calixarenes,[21-27] and pillar[n]arenes[28-29] also provides excellent selectivity and directionality with defined stoichiometry. Robust, reversible host–guest complexation with geometrically programmed valency is often orthogonal to other interactions, enabling the formation of sequence-controlled chains,[30-36] sequence-block architectures,[37-38] and cross-linked networks[39-40]. Supramolecular polymers based on host–guest complexes are particularly advantageous for achieving responsive behavior.[41] The affinity of host–guest complexes can be modulated by competitive guests or external stimuli, such as pH, ions, redox conditions, or light, enabling on-demand control of macroscopic

[a] Department of Chemistry, Graduate School of Advanced Science and Engineering, Hiroshima University, 1-3-1 Kagamiyama, Higashi-Hiroshima, Hiroshima 739-8526, Japan. E-mail: haino@hiroshima-u.ac.jp
[b] International Institute for Sustainability with Knotted Chiral Meta Matter (WPI-SKCM²), Hiroshima University, 1-3-1 Kagamiyama, Higashi-Hiroshima, Hiroshima, 739-8531, Japan.

ChemComm

View Article Online
DOI: 10.1039/D6CC02170K

Feature Article

properties through the formation and disruption of supramolecular polymer chains.[42-44]

1.2. Porphyrin-based supramolecular polymers

Porphyrins are versatile supramolecular scaffolds owing to their flat, aromatic macrocyclic structures and electron-rich nature.[45-46] However, π–π stacking between electron-rich porphyrin rings often provides insufficient stabilization to sustain polymer growth. Accordingly, porphyrin-based supramolecular polymerization typically requires orthogonal, directional noncovalent interactions that reinforce π–π stacking. A seminal prototype employed an amphiphilic porphyrin bearing water-soluble polyether side chains, which spontaneously formed cofacial assemblies in aqueous media.[47] Subsequent porphyrin assemblies relied on ionic and hydrophobic interactions,[48-49] together with π–π stacking,[50-52] to form fibrous supramolecular polymers (Fig. 2a).

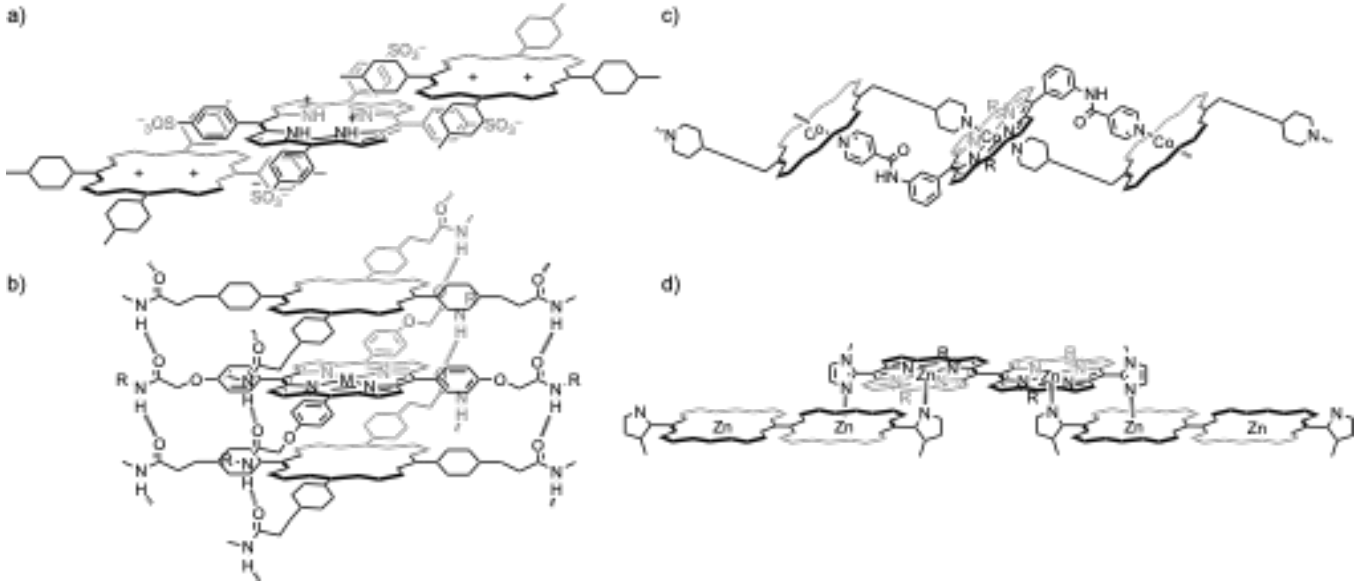

Fig. 2 Representative porphyrin-based supramolecular polymers.

Hydrogen bonding is a directional noncovalent interaction that promotes structural programmability in supramolecular polymerization. The highly directional head-to-tail hydrogen bonding between amide groups governs polymer growth perpendicular to the porphyrin surface, thereby facilitating π–π stacking (Fig. 2b).[53-57] Well-grown supramolecular polymers form gels in organic solvents. Cooperative growth (nucleation–elongation) is also achieved through the self-assembly of amide-functionalized porphyrins in lipophilic solvents. This cooperative mechanism enables living supramolecular polymerization, resulting in the synthesis of supramolecular block polymers.[58-60]

Metal–ligand coordination at metalloporphyrin cores provides a powerful alternative route to supramolecular porphyrin polymers. Because of its high directionality and strong binding, coordination-driven supramolecular polymerization yields structurally defined, highly stabilized supramolecular polymer chains.[61-62] Self-complementary dimerization of ligand-functionalized metalloporphyrins further enhances intermolecular association, facilitating long-chain growth (Fig. 2c,d).[63-67] Axial Zn–N multivalent coordination between multitopic porphyrins can also produce supramolecular polymers with a high degree of polymerization and chiral, layered architectures.[68-69]

Despite these advances, supramolecular polymers driven by host–guest complexation involving porphyrin-based host molecules remain less developed,[70] even though many porphyrin-based hosts exhibit strong molecular recognition.[71-76] This gap motivates the development of porphyrin-derived host architectures that combine a preorganized cavity with multiple recognition modes.

1.3. Supramolecular chemistry of bisporphyrin clefts

Bisporphyrin clefts are porphyrin dimers in which two porphyrin units are held at a defined distance and relative orientation by specific linkers. Consequently, bisporphyrin clefts function as electron-rich molecular tweezers that capture complementary guests within the cleft cavity.[77-79] The tunability of their geometry and electronic properties provides a programmable platform for molecular recognition in solution.

Historically, bisporphyrin clefts have served as powerful hosts for bidentate ligands and chiral guests.[80] In these clefts,

ChemComm

View Article Online
DOI: 10.1039/D6CC02170K

Feature Article

guest binding governs the cofacial arrangement and helical twist of the porphyrin pair, yielding sensitive chiroptical readouts via the circular dichroism (CD) exciton chirality method.[81-86] Furthermore, preorganization of the bisporphyrin cleft cavity improves binding strength and selectivity, enabling strong encapsulation of electron-deficient aromatics within the electron-rich cleft.[87]

Bisporphyrin clefts can provide multiple recognition modes within a single scaffold, a key attribute for supramolecular polymerization. In 2005, Haino et al. developed a pyridinedicarboxyamide-connected bisporphyrin cleft **1** (Fig. 3).[88] Bisporphyrin cleft **1** forms an uncommon head-to-head dimer **1•1** via complementary shape fitting, assisted by π–π stacking, CH/π, and hydrogen-bonding interactions.[89] In addition, the electron-rich cleft captures electron-deficient guests via π–π stacking and donor–acceptor interactions; for example, 2,4,7-trinitrofluorenone (**G1**) is strongly encapsulated within the cleft cavity.[90-91] Metallation at the N_4 cores further enables coordination-driven guest binding either at the cleft exterior or within the cavity. Monodentate guests coordinate from the cavity exterior to form a 1:2 host–guest complex, whereas shape complementarity promotes encapsulation of bidentate ligands within the cavity.[92-94] Accordingly, bisporphyrin cleft **1** offers three addressable recognition motifs—complementary dimerization, donor–acceptor host–guest binding, and metal coordination—that can be used separately, interchangeably, or simultaneously.

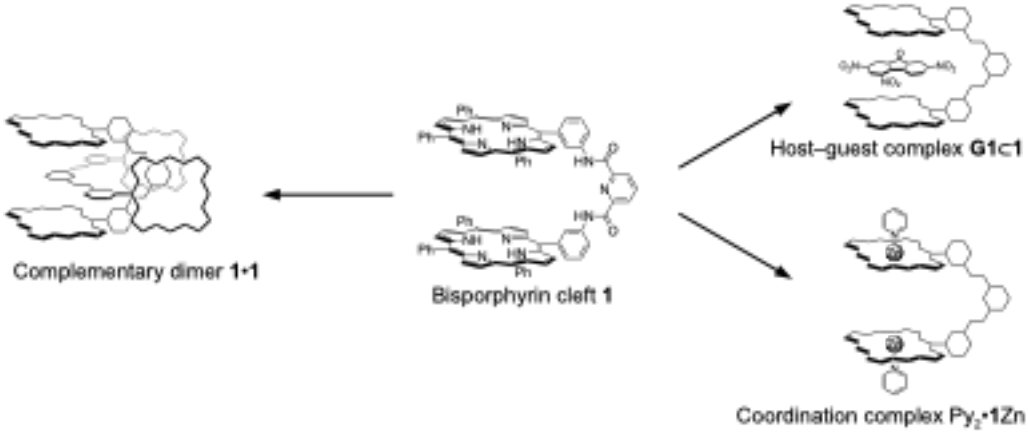

Fig. 3 Structures of a bisporphyrin cleft **1**, and its supramolecular complexes **1•1**, **G1⊂1**, and Py_2•**1**Zn.

Comparison of cleft **1** with conventional macrocyclic hosts and other bisporphyrin hosts reveals the significance of the three recognition motifs. Although conventional macrocycles provide well-defined cavities, the optical, chiroptical, or redox readouts of guest encapsulation often require additional reporting functionalities. In contrast, chromogenic, redox-active bisporphyrin clefts directly report and regulate the encapsulation of their guests within the binding cavities. Nevertheless, many bisporphyrin molecules are primarily utilized as hosts for the encapsulation of bidentate ligands or chiral analytes. In contrast, **1** can uniquely function as a repeat supramolecular junction with recognition pairs exchanged along the polymer backbone.

Considering **1** as a functional polymer junction, the following sections trace the translation of its recognition modes into supramolecular polymers and materials. The article proceeds from head-to-tail host–guest polymerization, ring–chain equilibria, and redox control to self-complementary dimerization, recognition-pair exchange, helicity control, chiral sensing, and finally, coordination-crosslinked gels and free-standing films.

2. Molecular recognition-directed supramolecular polymerization

2.1. Supramolecular polymerization directed by donor–acceptor host–guest complexation of bisporphyrin clefts

A common strategy for constructing supramolecular polymers uses a heterotopic monomer bearing a host unit at one terminus and a guest unit at the opposite terminus. The host–guest pair **G1⊂1** is well-suited to this design. In monomer **2**, a bisporphyrin cleft and a 4,5,7-trinitrofluorenone-2-carboxylate (TNF) unit are installed as the host and guest units, respectively (Fig. 4).[95] Head-to-tail host–guest complexation between the bisporphyrin cleft unit and the TNF unit drives supramolecular polymerization with a large association constant of 42,000 M^{-1}.

In general, supramolecular polymers exist in dynamic equilibrium with their monomeric species; thus, changes in monomer concentration directly affect the degree of polymerization that critically governs polymer properties. Therefore, determining the degree of polymerization (DP) at a given total monomer concentration (C_t) is essential. When

ChemComm

View Article Online
DOI: 10.1039/D6CC02170K

Feature Article

supramolecular polymerization follows isodesmic association, in which monomer association proceeds stepwise, the association constant (K) for each step is independent of the degree of polymerization. DP can be approximately estimated by $\mathrm{DP} = \sqrt{KC_t}$ in the regime where $\sqrt{4KC_t} \gg 1$; thus, the DP of poly-**2** is approximated as 122-mer at 60 mM.[96]

Although the DP of supramolecular polymers is difficult to determine experimentally, their hydrodynamic properties in solution can be evaluated as a function of concentration.[97] Accordingly, comparing the hydrodynamic radii (r_h) of a monomer and its supramolecular polymers provides a rough estimate of DP. Based on the Stokes–Einstein (SE) relation $D = k_B T/(6\pi\eta r_h)$, where k_B is the Boltzmann constant and η is the solvent viscosity, hydrodynamic volumes correlate with diffusion coefficients (Ds);[98] accordingly, the hydrodynamic ratio of a monomer and its aggregates is given by ($D_{monomer}$ / $D_{aggregate}$),[3] representing the DP of supramolecular polymers.[99] Diffusion coefficients in solution are determined by diffusion-ordered NMR spectroscopy (DOSY). The diffusion coefficient of **2** decreased markedly with increasing concentration. Using this relationship, the diffusion-coefficient ratio between monomeric **2** and its aggregate at 66 mM was 8.7, corresponding to a DP of 660-mer. By contrast, the association constant yields an estimated DP of 128-mer, which is lower than the DOSY-derived DP.

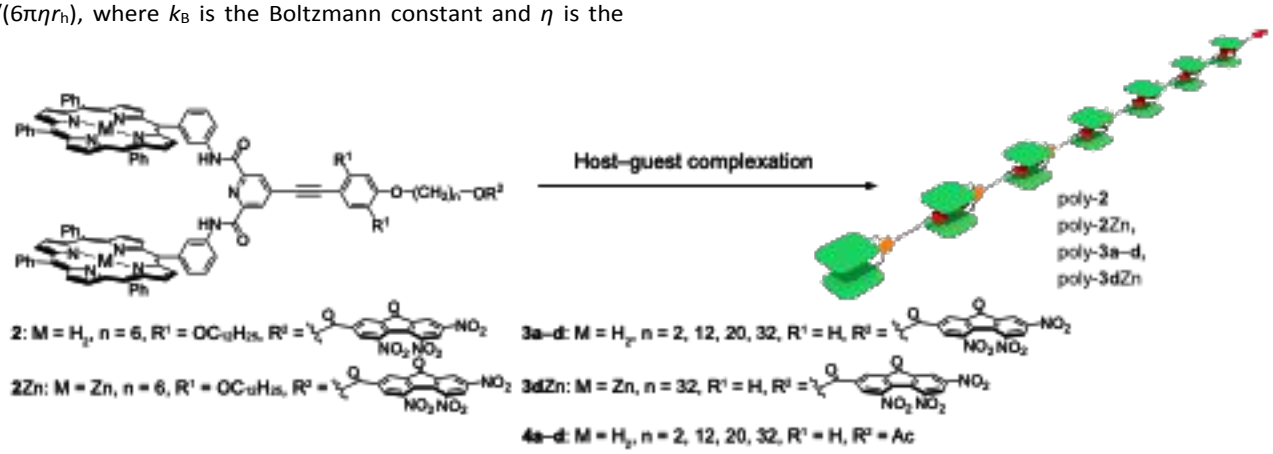

Fig. 4 Head-to-tail supramolecular polymerization driven by donor–acceptor host–guest complexation. Structures of heterotopic monomers **2**, **2**Zn, **3a–d**, and **3d**Zn, together with reference compounds **4a–d**.

The SE relation is most appropriate for compact, isotropic species in dilute solutions. Thus, the size difference between monomers and small oligomers at the early stages of supramolecular polymerization can be evaluated using the SE relation. As polymerization proceeds, however, the assemblies evolve into anisotropic, polymer-like structures, and a simple hard-sphere approximation may overestimate their apparent hydrodynamic volumes. Therefore, the discrepancy between the experimentally determined DP and that estimated from the association constant suggests deviations from spherical-particle behavior and may indicate formation of extended, potentially entangled supramolecular polymer structures in solution.

The solution dynamics of supramolecular polymers provide insights into polymer chain behavior. In poly-**2**, the polymeric chain structure is maintained by host–guest interactions and exists in dynamic equilibrium with monomer **2** on the experimental time scale. Nevertheless, time-averaged supramolecular polymer chains behave like conventional polymers in solution. In the dilute concentration regime, poly-**2** exhibits Rouse-like behavior. The critical polymerization concentration (CPC) in chloroform was observed at 24 mM, marking the transition from the dilute to the semi-dilute regime. Above CPC, the solution becomes more viscous, suggesting that chain relaxation follows Cates' mixed reptation–breakage regime,[100] in which supramolecular chains come into contact and become entangled, as commonly observed in polymer solutions.

Although isolated host–guest complexes typically exchange rapidly under dilute conditions, the mixed reptation–breakage regime in the entangled supramolecular polymer indicates that the relevant timescale is the effective persistence time of a host–guest junction within the chain. A junction continues to constrain chain motion until relaxation occurs through bond dissociation and/or exchange with a new partner. Accordingly, the effective junction persistence time is comparable to the reptation time. This persistence can be enhanced in an entangled medium through rapid rebinding to the original partner and restricted access to alternative binding partners in a crowded and entangled environment.

2.2. Ring–chain competition in supramolecular polymerization

ChemComm

View Article Online
DOI: 10.1039/D6CC02170K

Feature Article

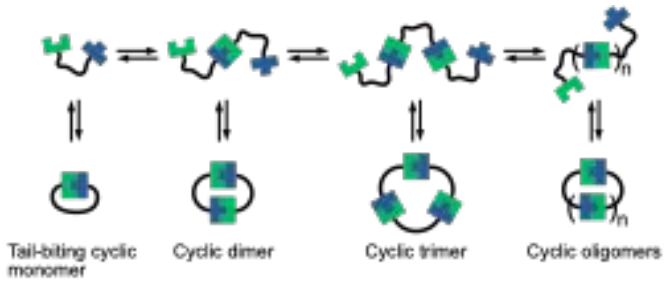

Fig. 5 Schematic of the ring–chain equilibrium in supramolecular polymerization.

The dynamic equilibrium between cyclic and linear polymeric chain structures has long been of interest in polymer science. The Jacobson–Stockmayer (JS) theory is a seminal model that describes this equilibrium in step-growth polymerization and predicts the statistical tendency of cyclization relative to chain growth.[101] Within the Gaussian-chain approximation, the formation of larger rings becomes progressively less probable with increasing ring size (n), resulting in an inverse power-law dependence of $\sim n^{-5/2}$, where n is the number of repeat units.

The JS theory has recently been broadened to supramolecular polymerization (Fig. 5). Within the JS framework, the ratio of the intramolecular association constant to the intermolecular association constant is referred to as the effective molarity (EM).[102-103] Therefore, EM quantifies the statistical preference for ring formation over chain formation within a given molecule.[104] Whitesides et al. examined how oligo(ethylene glycol) (EG□) linkers affect EM in an intramolecular protein–ligand complex, using a sulfonamide tethered to human carbonic anhydrase II. EM reached a maximum at an optimal linker length and decreased upon further elongation. These results were quantitatively described using a random-coil polymer model based on the JS theory. The flexible EG linkers retain substantial conformational mobility, and their effects are predominantly entropic, even when bound at both ends.

Meijer et al. investigated the supramolecular polymerization of AB-type protein monomers in which an S-peptide and an S-protein were tethered by flexible oligo(ethylene glycol) linkers of varying lengths.[105] Monomers with longer linkers closely followed JS predictions, and the product distribution was accurately described. In contrast, monomers with shorter linkers deviated from JS predictions at higher concentrations and preferentially formed cyclic monomers and dimers, indicating significant chain strain and a breakdown of the Gaussian-chain assumption inherent to the JS theory. They concluded that the JS theory provides a reliable quantitative description only when linker flexibility is sufficient to satisfy its statistical assumptions, thereby establishing design criteria for protein-based supramolecular polymers governed by ring–chain equilibria.

As supramolecular polymer design advances, EM-based approaches to interpret and tune the ring–chain equilibrium are essential for controlling polymer structure and material functionality, provided that non-ideal effects (e.g., the non-Gaussian behavior of short chains and transannular steric clashes) can be eliminated.[106] Accordingly, ring–chain equilibria in supramolecular polymers have been investigated experimentally using EM-based methods.[107-113]

Haino et al. focused on the contribution of non-ideal effects to the ring–chain equilibrium, which becomes apparent at the onset of supramolecular polymerization. In heterotopic monomers **3a–d**, step-growth supramolecular polymerization between the bisporphyrin cleft and the TNF unit competes with intramolecular cyclization, giving rise to a ring–chain equilibrium (Fig. 5).[114] Systematic variation of the linker chains connecting the bisporphyrin cleft and the TNF unit modulates the thermodynamic parameters—conformational enthalpy and entropy—that govern the ring–chain equilibrium. The CPC for supramolecular polymerization is influenced by these parameters, which vary with linker length. Below CPC, intramolecular cyclization occurs more frequently, whereas above CPC, intermolecular association predominates. The balance between these pathways is governed by conformational enthalpy and entropy and depends on linker flexibility. This systematic study of monomers **3a–d** provides a quantitative understanding of the conformational enthalpy and entropy associated with head-to-tail polymerization competing with cyclization.

At millimolar concentrations, the shorter linker chains in **3a**,**b** hindered intramolecular cyclization due to severe ring strains, thereby favoring intermolecular cyclic dimerization. In contrast, the longer linker chains in **3c**,**d** allowed intramolecular tail-biting cyclization. The intermolecular associations of **4a–d** provide the reference free-energy changes listed in Table 1. The free-energy changes for intermolecular cyclic dimerization of **3a**,**b** are comparable to those for the intermolecular associations of **4a**,**b**. By contrast, the free-energy changes for intramolecular cyclization of **3c**,**d** are smaller than those for the intermolecular interactions of **4c**,**d**. As described by the JS theory, both intra- and intermolecular cyclization suppress step-growth supramolecular polymerization. Accordingly, the longer alkyl chains in **3c**,**d** favor supramolecular polymerization and yield small EM values of 6.3×10^{-5} and 1.4×10^{-5} M. Conversely, the shorter linker chains in **3a**,**b** inhibit supramolecular polymerization.

ChemComm

View Article Online
DOI: 10.1039/D6CC02170K

Feature Article

Table 1 Association constants and thermodynamic parameters of cyclic dimerization of **3a**,**b**, intramolecular cyclization of **3c**,**d**, and intermolecular association of **4a–d**. Reproduced from ref.[114], copyright 2019, Macromolecules, American Chemical Society.

Monomer	K_{dim} / M^{-1}	ΔG° / kJ mol^{-1}	ΔH° / kJ mol^{-1}	$T\Delta S^\circ$ / kJ mol^{-1}	Monomer	Ka / M^{-1}	ΔG° / kJ mol^{-1}	ΔH° / kJ mol^{-1}	$T\Delta S^\circ$ / kJ mol^{-1}
3a	13.3×10^5	−35	−87	−54	**4a**	2.7×10^5	−31	−82	−52
3b	2.0×10^5	−30	−84	−51	**4b**	2.01×10^5	−30	−76	−46
Monomer	K_{iso}	ΔG° / kJ mol^{-1}	ΔH° / kJ mol^{-1}	$T\Delta S^\circ$ / kJ mol^{-1}	Monomer	Ka / M^{-1}	ΔG° / kJ mol^{-1}	ΔH° / kJ mol^{-1}	$T\Delta S^\circ$ / kJ mol^{-1}
3c	6.5	−3.8	−39	−36	**4c**	1.03×10^5	−28	−59	−30
3d	2.0	−1.7	−46	−45	**4d**	1.39×10^5	−29	−68	−39

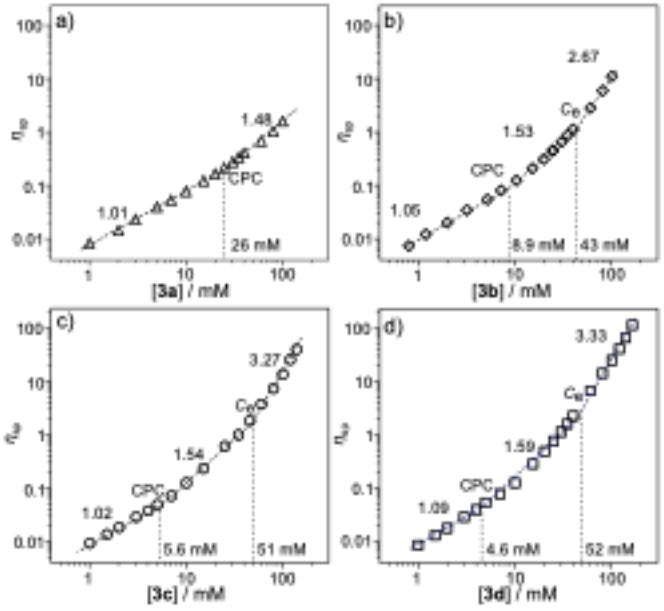

Fig. 6 Specific viscosity (η_{sp}) in chloroform at 25 °C versus concentration for (a) **3a**, (b) **3b**, (c) **3c**, and (d) **3d**. The slope values, CPC, and C_e are shown in each graph. Reproduced from ref.[114], copyright 2019, Macromolecules, American Chemical Society.

The thermodynamic parameters help explain the ring–chain equilibrium. The cyclization of **3a–d** provides an enthalpic gain but incurs a large entropic penalty. Each cyclic dimer of **3a**,**b** contains two host–guest complex motifs. Because host–guest complexation is enthalpically driven by donor–acceptor interactions, the enthalpy gain per host–guest motif in the cyclic dimers of **3a**,**b** is approximately half that of the intermolecular associations of **4a**,**b**, indicating the presence of ring strain in the cyclic dimers. Thus, intramolecular tail-biting cyclization of **3a**,**b** is disfavored due to intramolecular transannular strain. However, in the less strained tail-biting cyclic forms of **3c**,**d**, each host–guest motif largely retains the enthalpy gain observed for the corresponding intermolecular associations of **4c**,**d**. Accordingly, linker elongation relieves ring strain and facilitates intramolecular tail-biting cyclization in **3c**,**d**.

Entropy reflects multiple degrees of molecular freedom, including translational and rotational motion as well as internal vibrations and rotations around single bonds. Intermolecular association reduces translational freedom and therefore carries an entropic penalty. By contrast, unimolecular tail-biting cyclization is entropically more favorable with respect to translational entropy because it does not require loss of translational freedom. However, internal rotations around single bonds in flexible linker chains contribute substantially to conformational entropy, and tail-biting cyclization restricts these motions, imposing a significant conformational entropy cost. For **3c**,**d**, the conformational entropy costs of tail-biting cyclization are comparable to the translational entropy costs of intermolecular association (**3c**,**d** versus **4c**,**d**). Consequently, ring-opening polymerization of the tail-biting cyclic forms yields significant conformational entropy gains, which compensate for the translational entropy costs as supramolecular polymerization proceeds. This trade-off favors supramolecular polymerization of **3c**,**d**. Conversely, the shorter linkers in **3a**,**b** experience severe ring strain and therefore favor intermolecular cyclic dimerization, which avoids the large conformational entropy penalty associated with a long flexible linker chain. Consequently, the translational entropy costs associated with supramolecular polymerization of **3a**,**b** are not sufficiently compensated by conformational entropy gains upon ring opening of the cyclic dimers, thereby limiting the extent of polymer growth. Thus, conformational entropy is particularly important in the early stages of supramolecular polymerization, where intermolecular association must overcome a substantial translational entropy penalty.

The ring–chain equilibrium influences the progression of supramolecular polymerization. The solution dynamics of the supramolecular chains were strongly affected by the ring–chain equilibrium (Fig. 6). Monomers **3c**,**d** exhibited CPCs at lower concentrations than **3a**,**b**, indicating that longer linkers

ChemComm

View Article Online
DOI: 10.1039/D6CC02170K

Feature Article

facilitated supramolecular polymerization. Above CPCs, the scaling exponents (1.48–1.59) indicate that poly-**3a–d** exhibits Zimm-like behavior. For **3c**,**d**, which have flexible linker chains, an entangled concentration (C_e) was observed. Above C_e, the exponents exceeded 3, indicating that the supramolecular polymer chains came into contact and became entangled, most likely entering a mixed reptation–breakage regime. In contrast, intermolecular cyclic dimerization in poly-**3a**,**b** significantly increased CPCs and reduced the scaling exponent in poly-**3b** above C_e.

Accordingly, ring–chain competition primarily determines the equilibrium between the cyclic species and supramolecular linear chains, and the ring–chain transition is governed by conformational entropy arising from rotational freedom of the single bonds. A practical approach to assessing the contribution of rings to supramolecular polymerization is to measure specific viscosity. In the series of monomers **3a–d**, well-grown supramolecular chains are prone to flow under a mixed reptation–breakage regime, characterized by a scaling exponent exceeding 3.0. However, an increased contribution from cyclic species raises the CPC and reduces the scaling exponent above C_e. In this regime, substantial concentrations of cyclic oligomers decrease the concentration of well-grown supramolecular polymers and/or shorten the supramolecular chains, even at high overall concentration. Therefore, scaling exponents in supramolecular polymer solutions provide convenient indicators of the extent to which ring structures contribute to polymeric species. At a minimum, the emergence of an entanglement concentration C_e with scaling exponents exceeding 3.0 is crucial for forming sufficiently long supramolecular polymers. Finally, conformational entropy has a significant impact on the overall process of supramolecular polymerization.

2.3. Redox-responsive supramolecular polymerization

Reversible noncovalent interactions that preserve chain-like structures enable supramolecular polymer materials to adapt, self-correct, and respond to stimuli under mild conditions. Tuning the kinetic and thermodynamic stabilities of the noncovalent interactions that maintain supramolecular polymer chains enables stimulus-responsiveness and programmable viscoelasticity. Thus, supramolecular polymers are widely used in self-healing elastomers, responsive gels, recyclable plastics, and photo-responsive materials.[115-126] Solution concentration, temperature, pH, and light are common external stimuli that drive supramolecular polymers to grow or depolymerize. Among these stimuli, redox inputs alter the electron density of molecular building blocks, providing a convenient handle to regulate supramolecular polymerization and depolymerization. Developing a supramolecular polymer that can be depolymerized by either oxidation or reduction is therefore of particular interest for designing *dual* redox-regulated supramolecular materials.

Supramolecular polymer poly-**3d** is maintained by host–guest interaction between the bisporphyrin cleft and the TNF unit.[127] This interaction is governed by the electron density of the porphyrin rings and the electron deficiency of the TNF unit; therefore, redox modulation of the electronic properties of either component directly tunes the host–guest binding strength, thereby regulating the degree of supramolecular polymerization (Fig. 7).[128]

To enable reversible redox cycling, **3d** was converted to the zinc-metallated monomer **3d**Zn. Cyclic voltammetry showed reversible oxidation of the zinc porphyrins and reversible reduction of the TNF unit. One-electron oxidation of the porphyrin rings and one-electron reduction of the TNF unit, using tris(4-bromophenyl)aminium hexachloroantimonate (BAHA) and cobaltocene (CC), respectively, generated electron spin resonance-active cation and anion radicals that exhibited near-infrared absorption.

The zinc-metallated monomer **3d**Zn was self-assembled in 1,2-dichloroethane solution. The diffusion coefficient of **3d**Zn decreased threefold as its concentration increased to 31 mM, suggesting the formation of a substantial supramolecular polymer poly-**3d**Zn with a DP of 27. Chemical oxidation of the porphyrin rings and reduction of the TNF unit with BAHA and CC, respectively, perturbed supramolecular polymerization. Both oxidation and reduction increased the diffusion coefficient of poly-**3d**Zn, indicating that the redox treatments shortened the supramolecular polymer chains by weakening the host–guest interaction.

The solution dynamics were also influenced by the redox state. The specific viscosity of **3d**Zn exhibited a CPC of 10.3 mM. The slope of the log–log plot of specific viscosity versus concentration changed from 1.1 to 3.8 at the CPC. The supramolecular polymer chains displayed Zimm-like behavior below CPC, whereas they became entangled above it. Either chemical oxidation or reduction eliminated the characteristic CPC; accordingly, the supramolecular polymer chains were too short to allow chain–chain contact.

ChemComm

View Article Online
DOI: 10.1039/D6CC02170K

Feature Article

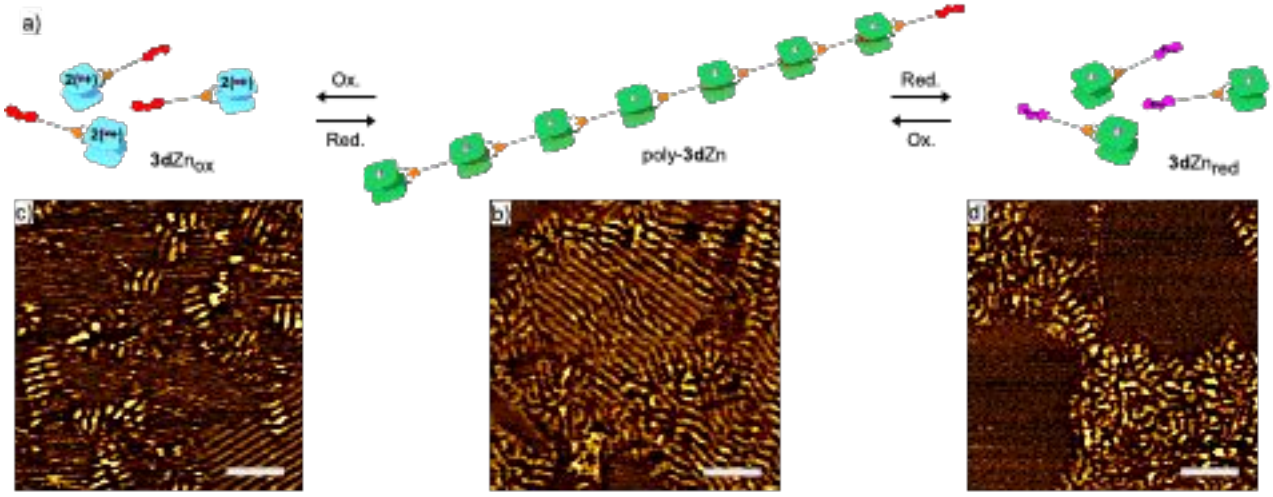

Fig. 7 (a) Schematic of redox-regulated supramolecular polymerization. (b–d) AFM images of spin-coated thin films of (b) **3d**Zn, (c) a 1:2 mixture of **3d**Zn and BAHA, and (d) a 1:1 mixture of **3d**Zn and CC, prepared from a 1,2-dichloroethane solution on HOPG. Scale bars, 50 nm. Adapted from ref.[127], copyright 2020, Chemical Communications, The Royal Society of Chemistry.

Atomic force microscopy (AFM) was used to visualize redox-triggered stretching and shrinking of the supramolecular polymer chains (Fig. 7b–d). Poly-**3d**Zn formed well-grown, long supramolecular chains with a height of 8.1 ± 1.3 nm and a length of 103 ± 37 nm. Given the 7.3 nm molecular dimension of monomer **3d**Zn, the DP of the supramolecular polymers is approximately 17 in the solid state. Redox perturbation of the host–guest complex with BAHA or CC shortened the supramolecular chains to 21 ± 8 and 19 ± 6 nm, respectively, supporting redox-triggered chain fragmentation and formation of shorter oligomers.

2.4. Post-polymerization modification of a supramolecular polymer formed by complementary dimerization of bisporphyrin cleft

The material properties of polymers are inherently influenced by their fundamental structures, including chain length, repeat-unit sequence, and monomer geometry. In copolymers, typical sequence structures include random, gradient, alternating, and block arrangements, which in turn dictate diverse morphologies and material properties. Achieving targeted material functions, therefore, requires control over copolymer sequence structure. Although main-chain modification is possible in dynamic covalent polymers, it remains difficult to achieve in a controlled manner in conventional polymers[129-131]

Constitutionally dynamic supramolecular polymers provide an unusual opportunity for post-polymerization modification of main-chain structure. In this approach, the supramolecular homopolymer poly-**5** is first formed via complementary dimerization of the bisporphyrin clefts and is then converted to a different chain structure through competing host–guest complexation (Fig. 8a). In this way, homopolymer poly-**5** is transformed into the supramolecular copolymer poly-**5**•**6** with an alternating monomer sequence.

Poly-**5** is fabricated through complementary dimerization of the bisporphyrin clefts.[132] Monomer **5** contains two bisporphyrin cleft units. Each cleft iteratively forms complementary dimers, thereby generating the supramolecular polymer poly-**5**. Self-assembly of **5** was promoted in 1,2-dichloroethane, with an association constant of 280,000 M^{-1}. As the concentration was increased to 30 mM, the hydrodynamic volume increased to 22-fold, indicating the formation of well-developed poly-**5**. These supramolecular polymers were responsive to competitive complexation with **G1**: the guest molecule completely disrupted the dimeric bisporphyrin cleft structure, forming a 2:1 host–guest complex (**G1**)$_2$⊂**5**.

ChemComm

View Article Online
DOI: 10.1039/D6CC02170K

Feature Article

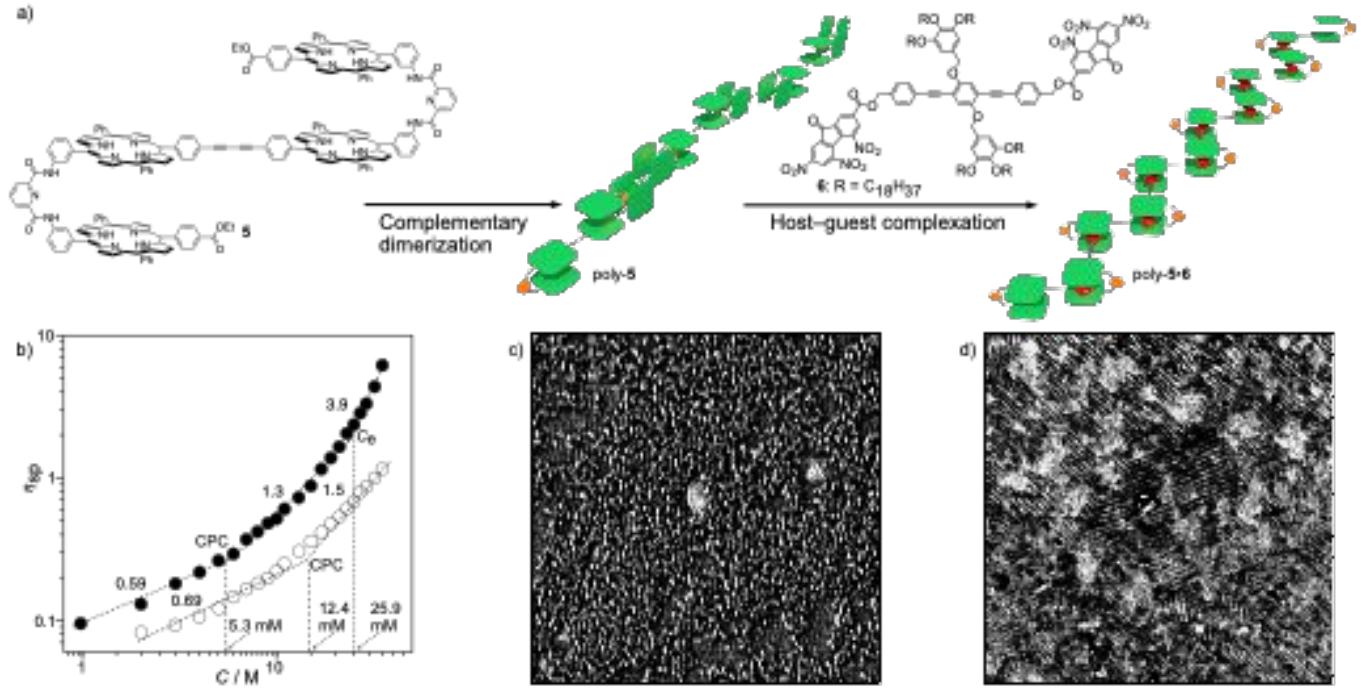

Fig. 8 (a) Schematic of supramolecular polymerization of tetrakisporphyrin **5** and in-chain modification by competitive complexation of ditopic guest **6**. (b) Log–log plots of specific viscosities for poly-**5** (open circles) and poly-**5•6** (filled circles). C denotes the total concentration of **5**. AFM images (500 × 500 nm) of (c) poly-**5** and (d) poly-**5•6** on HOPG. Reproduced from ref.[133], copyright 2018, Angewandte Chemie International Edition, VCH-Wiley.

The supramolecular polymer poly-**5** was dissociated by competitive complexation with the ditopic monomer **6**, converting the homopolymer sequence into an alternating monomer array.[133] This chain-structure conversion modulates macroscopic polymer properties. Upon addition of the ditopic monomer **6** to poly-**5**, the hydrodynamic volume of poly-**5** was gradually increased while the equivalent of **6** was below unity, consistent with enhanced hydrodynamic interactions arising from the long aliphatic side chains of **6**. However, an excess of **6** decreased the hydrodynamic volume, indicating dissociation of the supramolecular chains to form a 1:2 host–guest complex **5•6**$_2$. The transition from poly-**5** to poly-**5•6** occurred sharply at a 1:1 ratio of **5** and **6**, suggesting that formation of the alternating monomer structure in poly-**5•6** proceeds cooperatively.

Differences in chain rigidity influence the chain dynamics of the supramolecular polymers poly-**5** and poly-**5•6** (Fig. 8b). The TNF molecule encapsulated within the bisporphyrin cleft has in-plane rotational freedom, whereas the complementary bisporphyrin dimer is relatively rigid because of multiple noncovalent interactions. Accordingly, poly-**5** forms a comparatively rigid chain, whereas poly-**5•6** is more flexible. Above CPC, poly-**5** exhibited Zimm-like behavior without an entangled regime, implying that chain rigidity impedes entanglement. By contrast, poly-**5•6** displayed an entanglement concentration C_e, above which the flexible host–guest complex enabled clear chain entanglement, consistent with the Cates' mixed reptation–breakage regime.

In the solid state, conversion of homopolymer poly-**5** to the alternating monomer array in poly-**5•6** altered chain morphologies on HOPG (Fig. 8c,d). AFM revealed worm-like chains for poly-**5**, whereas poly-**5•6** formed highly ordered structures in which the supramolecular chains aligned within crystalline domains. The newly introduced octadecyl side chains of **6** likely promoted ordering of poly-**5•6** through interdigitation.

This dynamic control of monomer sequence via supramolecular chemistry—enabling transformation from a rigid rod-like chain to a flexible, entangled chain—offers a promising post-polymerization route to supramolecular polymers with uncommon sequences and distinct macroscopic properties.

3. Helicity-controlled supramolecular polymerization

Helical structures are widely recognized as fundamental patterns in nature, playing key roles in processes such as molecular recognition, catalysis, replication, and information

ChemComm

View Article Online
DOI: 10.1039/D6CC02170K

Feature Article

transfer across biological scales. Because elegant helical motifs, including α-helices and double-stranded nucleic acids, are ubiquitous, considerable effort has been devoted to creating artificial helical structures with defined handedness. Precise control of handedness in synthetic systems enables a broad range of potential applications, including memory, sensing, chiral stationary phases, asymmetric catalysis, and spin filtering.[134-137]

Unlike covalently linked helical polymers, helical supramolecular polymers can dynamically tune both chain length and helicity in response to external stimuli such as temperature, light, and pH. These dynamic features make helical supramolecular polymers advantageous for photoactive materials, catalysts, memory devices, and chiral sensors.[138-141]

3.1. Helical supramolecular porphyrin polymers directed by molecular recognition of bisporphyrin cleft

In-chain stereogenic units are typically effective in governing the handedness of helical supramolecular polymers. During chain formation via intermolecular host–guest complexation, monomers bearing stereogenic units can directly bias the preferred helical sense. Monomers (*R*)- and (*S*)-**7** contain a binaphthyl group as the stereogenic unit. The (*R*)- and (*S*)-configurations of the binaphthyl group drive the right-handed and left-handed helicities, respectively, of the helical supramolecular polymer poly-**7** (Fig. 9a). Although **7a** is structurally similar to **7b**, its supramolecular polymerization behavior differs from that of **7b**.

The self-assembly of **7a** produced a well-grown supramolecular polymer chain with a CPC of 6.0 mM and a C_e of 32.0 mM, whereas the supramolecular polymerization of **7b** was hindered by cyclic dimer formation and showed only a CPC of 15.0 mM.[142] Although the specific viscosities of both **7a** and **7b** indicated their CPCs, only **7a** exhibited a C_e. Above C_e, the supramolecular chains became entangled with a scaling exponent of 3.08, indicating that chain relaxation occurs in the mixed reptation–breakage regime.

Rigid monomer structures readily form cyclic oligomers without incurring a conformational entropy penalty, owing to their limited flexibility. Therefore, both **7a** and **7b** might appear unsuitable for supramolecular polymerization, as discussed in Section 2.2. However, the long, bulky alkyl side chains of **7a** become highly congested upon cyclic oligomer formation, thereby disfavoring ring closure. In contrast, the smaller alkyl side chains of **7b** can be accommodated within cyclic oligomers with minimal steric congestion, which facilitates ring formation. Thus, bulky side chains promote supramolecular polymerization by suppressing ring formation through steric clash.

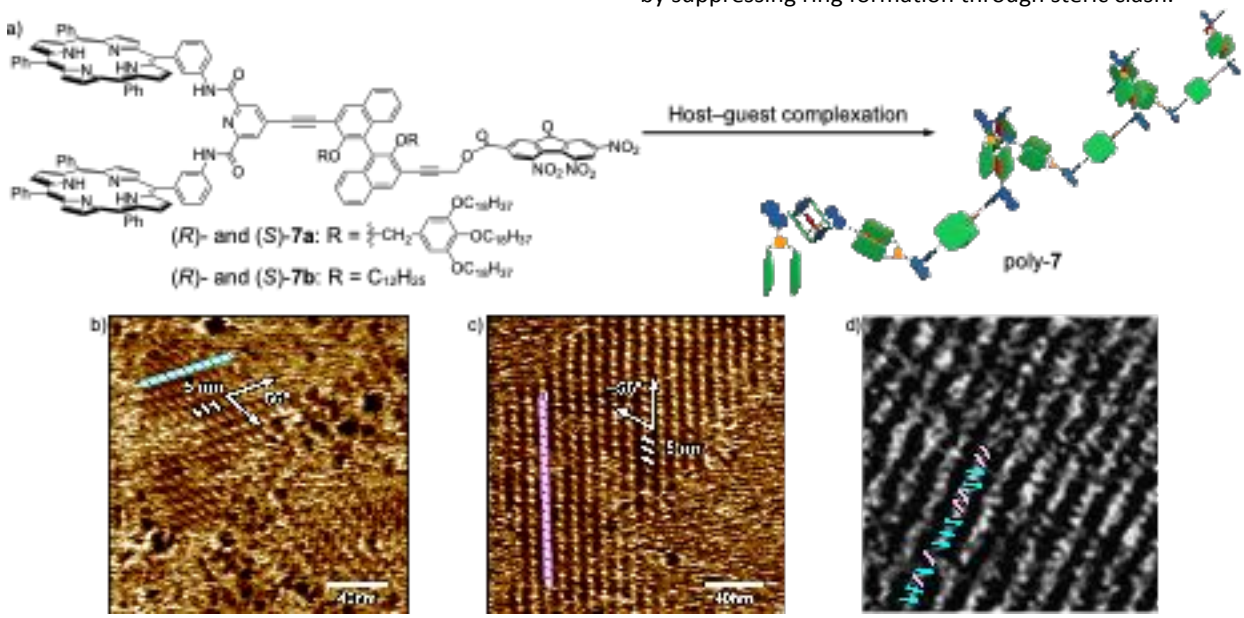

Fig. 9 (a) Helical supramolecular polymerization of the chiral monomers **7a**,**b**. AFM images of spin-coated films of (b) (*R*)-**7a**, (c) (*S*)-**7a**, and (d) a 1:1 mixture of (*R*)-**7a** and (*S*)-**7a** on HOPG. Reproduced from ref.[142] under the terms of the CC BY-NC 4.0 license.

The (*R*)- and (*S*)-configurations of the binaphthyl linkers bias the handedness of the helical supramolecular polymer chains, giving rise to bisignate circular dichroism in the Soret-band absorption of **7a**,**b**. In general, the CD signal most likely arises from the chirality of each repeating host–guest complex in the helical chain; therefore, CD alone is insufficient to determine the preferred helicity. AFM measurements of thin films of the helical supramolecular polymers on HOPG provide direct

ChemComm

View Article Online
DOI: 10.1039/D6CC02170K

Feature Article

evidence for determining helicity (Fig. 9b–d). Thin films prepared from (*R*)- and (*S*)-**7a** exhibited highly oriented crystalline domains with right-handed and left-handed helical morphologies, respectively. The periodic oblique strips are tilted by ±56° relative to the primary axis, with a pitch of 5 nm. Molecular modeling of the helical supramolecular polymer indicates that each helical segment consists of four molecular units of either (*R*)-**7a** or (*S*)-**7a**.

Supramolecular polymerization of a mixture of (*R*)- and (*S*)-**7a** can, in principle, yield either random or self-sorted supramolecular copolymers. To assess stereoselection in the polymer sequence, a 1:1 mixture of (*R*)- and (*S*)-**7a** was examined by AFM and was found to form uniform helical polymer chains. Both right-handed and left-handed helical twists coexisted within individual polymer chains, together with helical reversals. These observations indicate that the racemic mixture forms stereorandom helical supramolecular polymers without self-sorting behavior.

3.2. Helical supramolecular polymerization of chirally-twisted pseudo-macrocyclic tetrakisporphyrin

Tetrakisporphyrin **5** adopts an S-shaped conformation that drives helical supramolecular polymerization. However, because **5** lacks a stereogenic unit, right- and left-handed helical polymer structures coexist as a racemic mixture. Controlling handedness, therefore, requires the introduction of stereogenic units to bias the chiral conformation of **5**.[143] Newly designed tetrakisporphyrins **8a–d** bear amino acid side chains at each end (Fig. 10). Intramolecular end-to-end anti-parallel hydrogen bonding between the side chains maintains a pseudo-macrocyclic conformation. The α-substituents at the stereogenic centers are positioned outside the pseudo-macrocycle because of steric constraints, which influence the conformational preferences of both the right-handed (*P*) and left-handed (*M*) conformations. Consequently, self-assembly of the chirally twisted pseudo-macrocyclic monomers **8a–d** yields supramolecular pseudo-polycatenane polymers with controlled helicity.

The supramolecular polymerizations were strongly influenced by the bulkiness of the α-substituents. Increasing substituent size reduced the association constants and enthalpic gains of supramolecular polymerization. Because the two α-substituents are in close proximity in the pseudo-macrocyclic conformation, intramolecular steric interactions increase with substituent bulk. Accordingly, supramolecular polymer stability is inversely correlated with the bulkiness of the α-substituents.

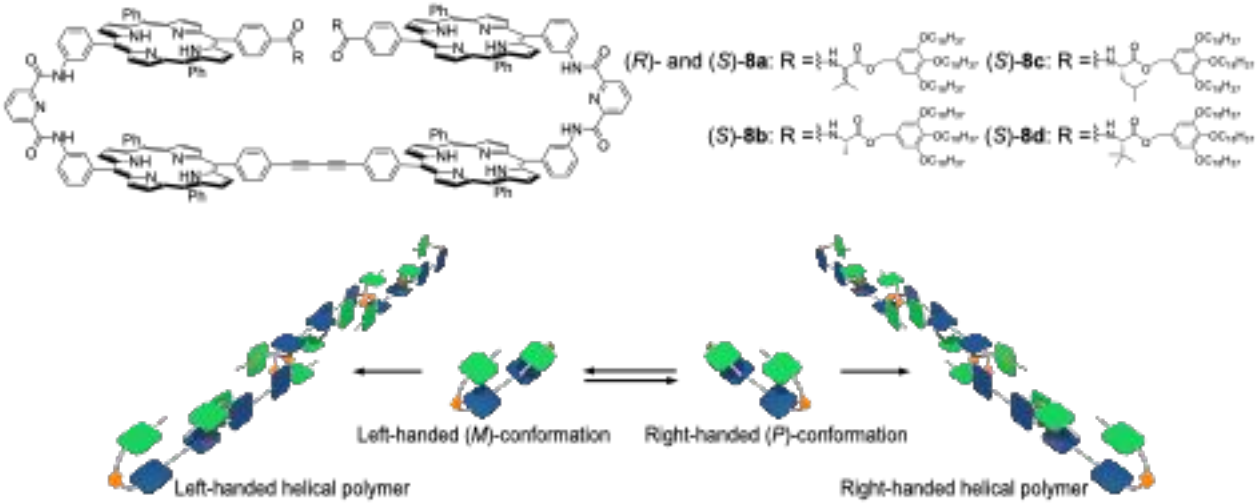

Fig. 10 Structures of **8a–d** monomers and schematic of supramolecular polymerization.

Helicity induction in the supramolecular pseudo-polycatenane polymers is governed by the bulkiness of the α-substituents. (*S*)- and (*R*)-**8a** displayed intense bisignate mirror CD signals in the Soret band, consistent with helical supramolecular polymers of preferred handedness (Fig. 11a). The bulkiness of the α-substituents influenced the CD intensities at 438 and 427 nm. Notably, introducing bulky *iso*- and *tert*-butyl groups markedly reduced the CD intensities, whereas the smallest methyl substituent enhanced the CD intensity. These results indicate that intramolecular steric interactions among the α-substituents control the preferred helicity of the supramolecular polymers.

AFM visualized the supramolecular pseudo-polycatenane polymer poly-(*S*)-**8a** (Fig. 11b). Well-developed supramolecular polymers were observed, with lengths of 13.6–361 nm and a uniform diameter of 6.9 ± 0.8 nm. Because the modeled oligomer structure yielded a repeat length of 2.7 nm and a width of 6.7 nm, the polymer chains correspond to approximately 5–134 monomer units. The nanostructured supramolecular polymer chains of poly-(*R*)-**8a** were successfully

ChemComm

View Article Online
DOI: 10.1039/D6CC02170K

Feature Article

generated, and right-handed helical polymers were clearly visualized with a pitch of 5.0 ± 0.4 nm (Fig. 11c). Considering the modeled repeat length of 2.7 nm, one helical turn comprised two monomer units. Oblique stripes were periodically oriented at a 45° angle relative to the primary axis of the polymer chain. Accordingly, these observations suggest that right- and left-handed helices in the supramolecular pseudo-polycatenane polymer arise from the conformations of the pseudo-macrocyclic monomers, which are dictated by the (*R*)- and (*S*)-configurations of the stereogenic centers, respectively.

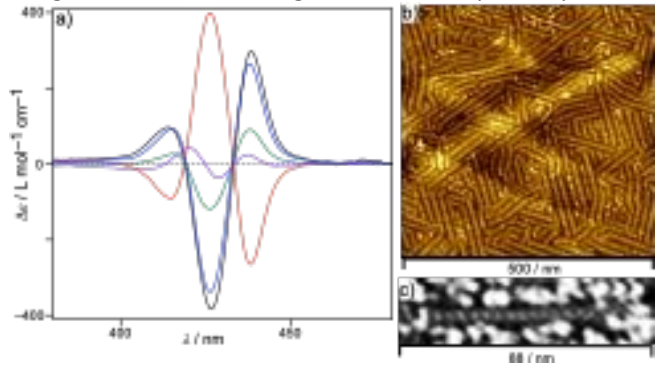

Fig. 11 (a) CD spectra of (*S*)-**8a** (blue), (*R*)-**8a** (red), (*S*)-**8b** (black), (*S*)-**8c** (green), and (*S*)-**8d** (purple) at a concentration of 5.0 × 10^{-2} mM in 1,2-dichloroethane at 298 K. (b,c) AFM images of (*S*)-**8a** (b) and (*R*)-**8a** (c). Adapted from ref.[143] under the terms of the CC BY-NC 4.0 license.

3.3. Sensing of solvent chirality by helical supramolecular polymer

Molecular sensors encompass a diverse range of molecules that undergo chromogenic or fluorogenic changes upon analyte binding. These spectral changes serve as readout signals detectable by spectroscopic methods and, in some cases, by visual inspection. CD spectroscopy is among the most widely employed techniques for determining the absolute configurations of chiral analytes; however, it is often of limited value for chiral molecules that lack appreciable absorption in the UV/vis region. Recent efforts have focused on developing advanced approaches utilizing chromogenic probes to determine the absolute configurations of non-chromogenic chiral molecules. Maeda, Yashima et al. used a π-conjugated helical poly(diphenylacetylene) as a colorimetric chiral sensor for chiral amines.[144] Non-racemic amines were covalently attached to the pendant carboxyl groups of a π-conjugated helical polyacetylene, and the resulting solutions displayed distinct colors depending on the analyte enantiomer, enabling naked-eye detection. Chromogenic hosts can also serve as sensors for cryptochiral analytes, including hydrocarbons, amines, amino alcohols, and amino acids.[145-146] Hong, Wang, Huang et al. reported that water-soluble pillar[n]arenes encapsulate cryptochiral guests, inducing chiral conformations in the hosts that produce strong enantiomer-dependent CD signals.[147] Encapsulation of cryptochiral amino acids and chiral secondary alcohols in the pillararene cavity produced diastereomeric host–guest complexes, resulting in induced CD effects that enabled readout of cryptochirality of the guest analytes.

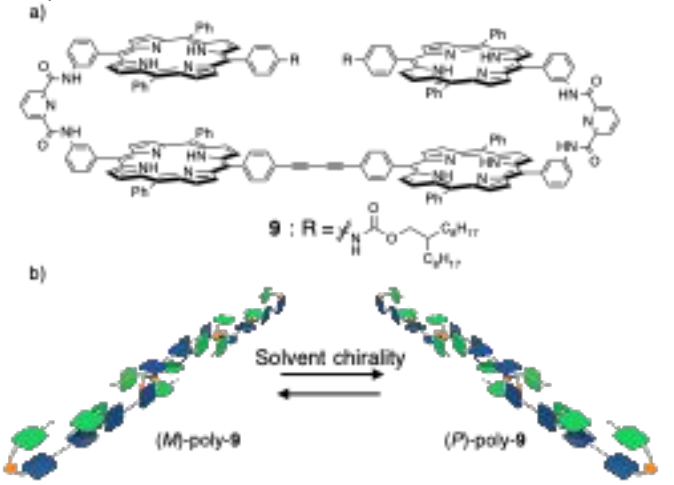

Fig. 12 (a) Molecular structures of tetrakis(porphyrin) **9**. (b) Schematic of the formation of the helical supramolecular polymer poly-**9**.

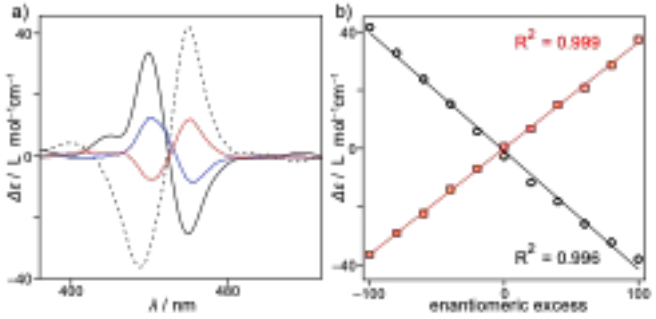

Fig. 13 (a) CD spectra of **9** (2.5 × 10^{-2} mM) in (red) (+)-limonene, (blue) (–)-limonene, (dashed line) (–)-α-pinene, and (solid line) (–)-β-pinene at room temperature. (b) Linear correlation between the ee and Δε values of **9** (2.5 × 10^{-2} mM) at (red) 422 nm and (black) 437 nm in α-pinene. Adapted from ref.[148] under the terms of the CC BY-NC 3.0 license.

Supramolecular polymer chemistry offers a distinct and straightforward strategy for extracting otherwise hidden chiral information from chiral molecules using CD probes. Achiral tetrakisporphyrin **9** forms supramolecular polymers comprising right- and left-handed helices in a 1:1 ratio.[148-149] The helical sense of poly-**9** is biased by external chirality, with the CD sign of the porphyrin Soret band serving as the chiroptical readout (Fig. 12).

Limonene is a typical non-chromogenic chiral molecule. Its lipophilic nature facilitated the supramolecular polymerization of **9**, increasing the association constant to 1.2 × 10^{7} M^{-1} at 90 °C. Consequently, limonene promoted the formation of poly-

ChemComm

View Article Online
DOI: 10.1039/D6CC02170K

Feature Article

9, most likely affording a high degree of polymerization at ambient temperature and thereby enhancing the sensitivity of the readout to solvent chirality. When **9** was dissolved in (+)- and (–)-limonene, intense mirror-image CD signals appeared at the Soret band (Fig. 13). Because limonene exhibits negligible absorption in the visible range, the CD response was attributed to chirality transfer from the solvent to the racemic helical supramolecular polymer poly-**9**. Based on the CD signs, left-handed and right-handed helical structures formed in (+)- and (–)-limonene, respectively. In (–)-α-pinene, the left-handed helical structure was more pronounced, whereas (–)-β-pinene induced a right-handed helical structure. Thus, the position of the double bond in pinenes is highly sensitive in determining the handedness of poly-**9**. A strong linear correlation ($R^2 > 0.995$) between the CD intensities at 422 and 437 nm and the enantiomeric excess (ee) of α-pinene enabled accurate ee quantification. For (+)/(–)-α-pinene mixtures of known composition, ee values estimated from Δε at 422 nm agreed with the true values within 4%, demonstrating that poly-**9** is an effective chiral sensor.

4. Supramolecular polymer materials

Supramolecular polymers rely on various noncovalent interactions. However, their practical use may be limited by poor mechanical robustness, owing to the reversible nature of noncovalent bonds. To address the limited robustness of linear supramolecular polymers derived from molecular monomers, monomer designs often incorporate multiple complementary interaction sites. In practice, two or more binding functionalities are introduced per monomer. Such supramolecular polymerization can produce interconnected networks, imparting macroscopic robustness to supramolecular materials.

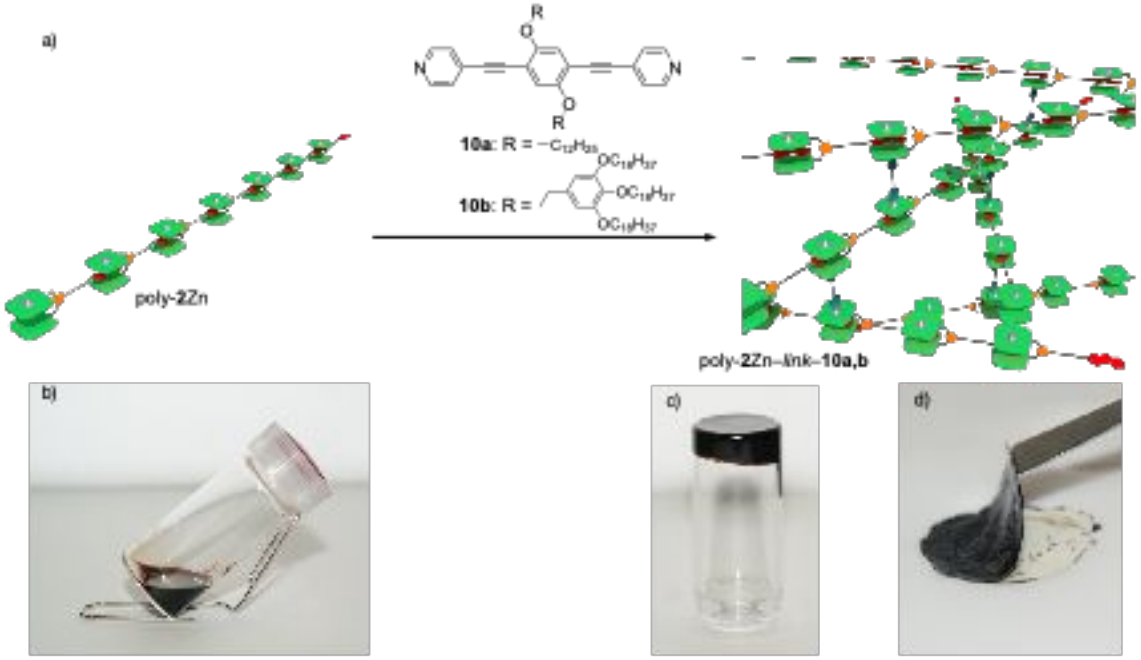

Fig. 14 (a) Schematic of the cross-linking of the supramolecular polymer poly-**2**Zn with **10**. Photographs of (b) a solution of **2**Zn (18 wt%) and (c) a gel of **2**Zn with 1.0 equiv. of **10b** (18 wt%) in 1,1,2,2-tetrachloroethane. (d) A free-standing film prepared from a chloroform solution of **2**Zn with 1 eq. of **10b**. Reproduced from ref.[150], copyright 2015, Angewandte Chemie International Edition, VCH-Wiley.

An early attempt to develop mechanically robust supramolecular materials was reported by Meijer et al.[151] They used 2-ureido-4-pyrimidone (UPy), which forms a self-complementary dimer with a dimerization constant exceeding six orders of magnitude. Polydimethylsiloxane bearing UPy units at each chain end exhibited shear-thinning behavior and a strong temperature-dependent viscosity. This thermoplastic behavior was attributed to the dissociation of the noncovalent bonds at high temperatures. Rebek et al. demonstrated that reversibly self-assembled, hydrogen-bonded polycaps exhibit mechanical integrity and viscoelasticity comparable to those of covalent polymers, while maintaining substantial physical strength.[152] These reversible properties enable the formation of high-strength recyclable fibers and responsive gels that can be controlled by chemical or thermal stimuli. Weder et al. developed supramolecular polymer networks based on the self-assembly of UPy-functionalized tris(hydroxymethyl)propane.[153] These materials were robust, with a storage modulus of 3.65 GPa at room temperature, and exhibited high stiffness in the glassy regime at ambient temperature. Moreover, scratches

ChemComm

View Article Online
DOI: 10.1039/D6CC02170K

Feature Article

healed upon UV exposure. UV absorption by the UPy units converted light to heat, enabling rapid healing. Collectively, these studies underscore the key role of multidentate monomer structures in producing mechanically robust supramolecular polymer materials.

Haino et al. developed supramolecular polymer materials based on the molecular recognition within the bisporphyrin cleft. In bulk, the supramolecular polymer poly-**2** (M = H_2) is insufficiently robust to fabricate free-standing films.[150] Incorporation of a zinc ion into the porphyrin core introduces coordination sites, creating additional interaction sites through coordination of the linker nitrogens in **10a**,**b** (Fig. 14). This coordination-mediated cross-linking of poly-**2**Zn (M = Zn) provides a practical route to supramolecular materials with macroscopic mechanical integrity.

The zinc porphyrin rings of **2**Zn did not affect self-association, with an association constant of 240,000 M^{-1}. The supramolecular polymerization of **2**Zn decreased its diffusion coefficient threefold, indicating that the DP of poly-**2**Zn exceeded 27 at millimolar concentrations. The addition of a 0.5-equivalent amount of **10a** to poly-**2**Zn further decreased the diffusion coefficient, indicating that coordination cross-linking converts the supramolecular chain structure of poly-**2**Zn into the networked supramolecular polymer poly-**2**Zn•**10a**.

The effect of **10b** is most evident in the rheological response. Adding **10b** lowered the CPC of poly-**2**Zn to 14.5 mM. Above this CPC, the cross-linker created effective interchain connections among the poly-**2**Zn supramolecular polymers, producing a sharp upturn that indicates formation of a highly interconnected supramolecular polymer network, poly-**2**Zn•**10b**.

The solution dynamics of the poly-**2**Zn supramolecular polymer networks with **10b** were characterized by dynamic viscoelastic measurements. At low frequencies, the storage and loss moduli (G' and G'') scaled as ω^2 and ω^1, respectively, consistent with relaxation governed by a single terminal relaxation time. Network relaxation is therefore governed primarily by the breaking and reforming of the noncovalent bonds that define both the polymer backbone and junction points, although these interactions could, in principle, contribute independently. In general, individual noncovalent links are shorter-lived than the terminal relaxation time of the network. However, the poly-**2**Zn•**10b** network is highly entangled, which may extend effective bond lifetimes through steric crowding at intermonomer connections and junction sites.

The distinctive chain dynamics of the supramolecular polymer network poly-**2**Zn•**10b** translate into substantially improved bulk properties. The purple 1,1,2,2-tetrachloroethane solution of **2**Zn became viscous and gelled upon addition of **10b**. The solution was concentrated onto a Teflon sheet, forming a free-standing film that exhibited flexibility with a Young's modulus of 1 GPa. Although the poly-**2**Zn•**10b** network is built from molecular monomers linked by noncovalent bonds, the resulting supramolecular polymer materials were stable and displayed unexpectedly high mechanical robustness.

5. Conclusions and outlook

Bisporphyrin clefts—rigidly linked porphyrin dimers that act as electron-rich molecular tweezers—combine three addressable recognition modes (donor–acceptor host–guest binding, self-complementary dimerization, and metal coordination) into a modular platform for supramolecular polymerization. The step-growth head-to-tail assembly of heterotopic monomers affords supramolecular polymer chains with a high degree of polymerization, with their topology and length governed by ring–chain equilibria encoded by linker conformational entropy. The electronically tunable donor–acceptor interaction further enables redox-controlled modulation of chain length and viscoelasticity. Interchangeable recognition motifs permit post-polymerization main-chain editing, while stereogenic elements or chiral media bias helicity and amplify chiroptical responses. The integration of host–guest backbones with orthogonal coordination cross-links has been shown to convert dynamic chains into robust supramolecular networks and free-standing films.

The demonstrated functions of bisporphyrin-cleft-based complexes, polymers, and networks point to several application-oriented directions. Redox-modulated donor–acceptor recognition allows switchable control over chain length, viscosity, and entanglement. Recognition-pair exchange provides a route to reconfigurable supramolecular copolymers in which sequence, rigidity, and mesoscale ordering can be modified. Helicity amplification translates weak or cryptic solvent chirality into intense CD outputs, enabling chiral sensing and enantiomeric excess analysis. Coordination crosslinking converts molecularly defined recognition motifs to gels and mechanically robust films. Together, these examples establish design principles for responsive soft materials, chiral optical sensors, and recyclable supramolecular polymer networks.

Several fundamental challenges must be overcome before bisporphyrin-cleft-based supramolecular polymers can be controlled with the same precision as covalent polymers or kinetically controlled supramolecular polymers. The cleft-based chain growth described thus far largely relies on thermodynamically controlled step-growth association, where the degree of polymerization and chain-length distribution are dictated by association equilibria, concentration, and stoichiometric balance rather than by controlled initiation and

ChemComm

View Article Online
DOI: 10.1039/D6CC02170K

Feature Article

propagation. This intrinsic equilibrium makes it difficult to regulate dispersity, end-group fidelity, and sequence uniformity with high precision. Ring–chain competition further complicates polymer growth by diverting monomers into cyclic species, increasing the CPC, reducing the population of long linear polymer chains, and weakening the onset of chain entanglement. Although recognition-pair exchange enables attractive post-polymerization main-chain editing, the dynamic host–guest junctions that facilitate such modifications also impede the incorporation of living-like characteristics, including controlled initiation, seeded elongation, chain-end memory, and narrow dispersity. The labile host–guest interactions provide responsiveness, stress relaxation, and adaptivity; however, they can limit load transfer, fracture resistance, and long-term shape persistence. Therefore, an unresolved challenge in the field of supramolecular polymer materials is to progress beyond stiffness and impart toughness to the polymers by balancing reversible energy dissipation with persistent network connectivity.

Beyond these drawbacks, bisporphyrin clefts provide opportunities that are difficult to access with conventional macrocyclic hosts or purely hydrogen-bonded supramolecular polymers, because a chromophoric, redox-active, and coordinatively addressable recognition unit is directly embedded in the polymer backbone. Kinetically programmed cleft assembly could lead to supramolecular analogs of sequence-defined or block polymers, in which chain length, sequence, and helicity are controlled by seeded growth and subsequently modified by recognition-pair exchange. The coexistence of donor–acceptor binding, self-complementary dimerization, and metal coordination may also enable the formation of multi-input polymers that transduce chemical, redox, chiral, and mechanical stimuli into coupled changes in chain length, viscoelasticity, CD, and network connectivity. Helically organized porphyrin arrays are attractive candidates for chiral optical materials and sensing platforms, while redox-active clefts and coordination nodes can be used to organize dynamic chains into anisotropic, hierarchically ordered materials. In soft materials, combining labile host–guest junctions with longer-lived coordination crosslinks, entanglements, or phase-organized domains would yield tough, self-healing, reprocessable films and gels whose optical and mechanical properties can be tuned by orthogonal stimuli. These directions would move bisporphyrin-cleft-based polymers toward adaptive and functionally programmable soft matter.

Data availability

No new data were created in the course of preparing this manuscript. All the data sources mentioned in the article are publicly accessible and have been properly cited.

Author contributions

The manuscript was collaboratively written by all authors, who also approved its final version. The authors utilized ChatGPT, Paperpal, and Grammarly to improve language and readability in the manuscript. The authors reviewed and edited the output, and they take full responsibility for the content of the publication.

Conflicts of interest

There are no conflicts to declare.

Acknowledgements

This work was supported by JSPS KAKENHI Grant-in-Aid for Transformative Research Areas (A), "Materials Science of Meso-Hierarchy" (Grant No. JP23H04873), Grant-in-Aid for Transformative Research Areas (A), "The Pursuit of Functionality Woven by π-Molecular Complexity" (Grant No. 26H01360), and Grants-in-Aid for Scientific Research (A), (B), and (C) (Grant Nos. JP25H00897, 25K01754, and 25K18021). TH acknowledges funding from the Amano Institute of Technology Foundation, the Izumi Science and Technology Foundation, the Iwatani Naoji Foundation, and the Urakami Foundation.

Notes and references

1 L. Brunsveld, B. J. B. Folmer, E. W. Meijer and R. P. Sijbesma, *Chem. Rev.*, 2001, **101**, 4071-4097.
2 H. M. Keizer and R. P. Sijbesma, *Chem. Soc. Rev.*, 2005, **34**, 226-234.
3 N. Roy, V. Schädler and J. M. Lehn, *Acc. Chem. Res.*, 2024, **57**, 349-361.
4 T. Haino, *Polym. J.*, 2013, **45**, 363-383.
5 S. K. Yang, A. V. Ambade and M. Weck, *Chem. Soc. Rev.*, 2011, **40**, 129-137.
6 B. Adhikari, X. Lin, M. Yamauchi, H. Ouchi, K. Aratsu and S. Yagai, *Chem. Commun.*, 2017, **53**, 9663-9683.
7 Y. Liu, L. Wang, L. Zhao, Y. Zhang, Z.-T. Li and F. Huang, *Chem. Soc. Rev.*, 2024, **53**, 1592-1623.
8 C. Fouquey, J.-M. Lehn and A.-M. Levelut, *Adv. Mater.*, 1990, **2**, 254-257.
9 R. K. Castellano, D. M. Rudkevich and J. Rebek, Jr., *Proc. Natl. Acad. Sci. USA*, 1997, **94**, 7132-7137.
10 H. A. Klok, K. A. Jolliffe, C. L. Schauer, L. J. Prins, J. P. Spatz, M. Moller, P. Timmerman and D. N. Reinhoudt, *J. Am. Chem. Soc.*, 1999, **121**, 7154-7155.
11 B. J. B. Folmer, R. P. Sijbesma, R. M. Versteegen, J. A. J. van der Rijt and E. W. Meijer, *Adv. Mater.*, 2000, **12**, 874-878.
12 S. Yagai, T. Nakajima, K. Kishikawa, S. Kohmoto, T. Karatsu and A. Kitamura, *J. Am. Chem. Soc.*, 2005, **127**, 11134-11139.
13 N. Yamaguchi, D. S. Nagvekar and H. W. Gibson, *Angew. Chem. Int. Ed.*, 1998, **37**, 2361-2364.
14 N. Yamaguchi and H. W. Gibson, *Angew. Chem. Int. Ed.*, 1999, **38**, 143-147.

ChemComm

View Article Online
DOI: 10.1039/D6CC02170K

15 H. W. Gibson, N. Yamaguchi and J. W. Jones, *J. Am. Chem. Soc.*, 2003, **125**, 3522-3533.
16 M. Miyauchi and A. Harada, *J. Am. Chem. Soc.*, 2004, **126**, 11418-11419.
17 M. Miyauchi, T. Hoshino, H. Yamaguchi, S. Kamitori and A. Harada, *J. Am. Chem. Soc.*, 2005, **127**, 2034-2035.
18 A. Harada, R. Kobayashi, Y. Takashima, A. Hashidzume and H. Yamaguchi, *Nat. Chem.*, 2011, **3**, 34-37.
19 G. Li and L. B. Mcgown, *Science*, 1994, **264**, 249-251.
20 Y. L. Liu, Y. Yu, J. A. Gao, Z. Q. Wang and X. Zhang, *Angew. Chem. Int. Ed.*, 2010, **49**, 6576-6579.
21 M. F. Parisi, D. Garozzo, G. Gattuso, F. H. Kohnke, A. Notti, S. Pappalardo, I. Pisagatti, A. J. P. White and D. J. Williams, *Org. Lett.*, 2003, **5**, 4025-4028.
22 T. Haino, Y. Matsumoto and Y. Fukazawa, *J. Am. Chem. Soc.*, 2005, **127**, 8936-8937.
23 Y. Cohen, S. Pappalardo, V. Villari, S. Slovak, G. Gattuso, A. Notti, A. Pappalardo, I. Pisagatti and M. R. Parisi, *Chem. Eur. J.*, 2007, **13**, 8164-8173.
24 E. Dalcanale, R. M. Yebeutchou, F. Tancini, N. Demitri, S. Geremia and R. Mendichi, *Angew. Chem. Int. Ed.*, 2008, **47**, 4504-4508.
25 F. Tancini, R. M. Yebeutchou, L. Pirondini, R. De Zorzi, S. Geremia, O. A. Scherman and E. Dalcanale, *Chem. Eur. J.*, 2010, **16**, 14313-14321.
26 T. Hirao, Y. Iwabe, N. Fujii and T. Haino, *J. Am. Chem. Soc.*, 2021, **143**, 4339-4345.
27 K. Hamada, D. Shimoyama, T. Hirao and T. Haino, *Bull. Chem. Soc. Jpn.*, 2022, **95**, 621-627.
28 Z. Zhang, Y. Luo, J. Chen, S. Dong, Y. Yu, Z. Ma and F. Huang, *Angew. Chem. Int. Ed.*, 2011, **50**, 1397-1401.
29 T. Ogoshi, T. Furuta and T. Yamagishi, *Chem. Commun.*, 2016, **52**, 10775-10778.
30 F. Wang, C. Y. Han, C. L. He, Q. Z. Zhou, J. Q. Zhang, C. Wang, N. Li and F. H. Huang, *J. Am. Chem. Soc.*, 2008, **130**, 11254-11255.
31 Z. B. Niu, F. H. Huang and H. W. Gibson, *J. Am. Chem. Soc.*, 2011, **133**, 2836-2839.
32 T. Ogoshi, H. Kayama, D. Yamafuji, T. Aoki and T. Yamagishi, *Chem. Sci.*, 2012, **3**, 3221-3226.
33 Z. H. Huang, L. L. Yang, Y. L. Liu, Z. Q. Wang, O. A. Scherman and X. Zhang, *Angew. Chem. Int. Ed.*, 2014, **53**, 5351-5355.
34 T. Hirao, H. Kudo, T. Amimoto and T. Haino, *Nat. Commun.*, 2017, **8**, 634.
35 T. Hirao, N. Fujii, Y. Iwabe and T. Haino, *Chem. Commun.*, 2021, **57**, 11831-11834.
36 C. Y. Ma, S. Ohtani, W. H. Wang, K. Kato, S. D. Zhang and T. Ogoshi, *Chem. Eur. J.*, 2025, **31**, e02040.
37 T. Park and S. C. Zimmerman, *J. Am. Chem. Soc.*, 2006, **128**, 13986-13987.
38 S. K. Yang, A. V. Ambade and M. Weck, *J. Am. Chem. Soc.*, 2010, **132**, 1637-1645.
39 H. Xu and D. M. Rudkevich, *Chem. Eur. J.*, 2004, **10**, 5432-5442.
40 F. Wang, J. Zhang, X. Ding, S. Dong, M. Liu, B. Zheng, S. Li, L. Wu, Y. Yu, H. W. Gibson and F. Huang, *Angew. Chem. Int. Ed.*, 2010, **49**, 1090-1094.
41 T. Haino, *Chem. Rec.*, 2015, **15**, 837-853.
42 X. Yan, F. Wang, B. Zheng and F. Huang, *Chem. Soc. Rev.*, 2012, **41**, 6042-6065.
43 D. Liu, G. Yin, X. Le and T. Chen, *Polym. Chem.*, 2022, **13**, 1940-1952.
44 S. Wang, P. J. Ong, S. Liu, W. Thitsartarn, M. J. B. H. Tan, A. Suwardi, Q. Zhu and X. J. Loh, *Chem. Asian J.*, 2022, **17**, e202200608.
45 J. Weiss, *J. Incl. Phenom. Macro.*, 2001, **40**, 1-22.
46 S. S. Santhosh Babu and D. Bonifazi, *ChemPlusChem*, 2014, **79**, 895-906.
47 T. Aida, A. Takemura, M. Fuse and S. Inoue, *J. Chem. Soc., Chem. Commun.*, 1988, 391-393.
48 T. Komatsu, K. Nakao, H. Nishide and E. Tsuchida, *J. Chem. Soc., Chem. Commun.*, 1993, **29**, 728-730.
49 J. M. Ribo, J. Crusats, J. A. Farrera and M. L. Valero, *J. Chem. Soc., Chem. Commun.*, 1994, **30**, 681-682.
50 P. D. W. Boyd, M. C. Hodgson, C. E. F. Rickard, A. G. Oliver, L. Chaker, P. J. Brothers, R. D. Bolskar, F. S. Tham and C. A. Reed, *J. Am. Chem. Soc.*, 1999, **121**, 10487-10495.
51 M. Wolffs, F. J. M. Hoeben, E. H. A. Beckers, A. P. H. J. Schenning and E. W. Meijer, *J. Am. Chem. Soc.*, 2005, **127**, 13484-13485.
52 Y. Hizume, K. Tashiro, R. Charvet, Y. Yamamoto, A. Saeki, S. Seki and T. Aida, *J. Am. Chem. Soc.*, 2010, **132**, 6628-6629.
53 M. Shirakawa, N. Fujita and S. Shinkai, *J. Am. Chem. Soc.*, 2005, **127**, 4164-4165.
54 R. van Hameren, A. M. van Buul, M. A. Castriciano, V. Villari, N. Micali, P. Schon, S. Speller, L. M. Scolaro, A. E. Rowan, J. A. A. W. Elemans and R. J. M. Nolte, *Nano Lett.*, 2008, **8**, 253-259.
55 F. Helmich, C. C. Lee, M. M. L. Nieuwenhuizen, J. C. Gielen, P. C. M. Christianen, A. Larsen, G. Fytas, P. E. L. G. Leclère, A. P. H. J. Schenning and E. W. Meijer, *Angew. Chem. Int. Ed.*, 2010, **49**, 3939-3942.
56 K. V. Rao, D. Miyajima, A. Nihonyanagi and T. Aida, *Nat. Chem.*, 2017, **9**, 1133-1139.
57 Z. L. Li, C. J. Zeman, S. R. Valandro, J. P. O. Bantang and K. S. Schanze, *J. Am. Chem. Soc.*, 2019, **141**, 12610-12618.
58 S. Ogi, K. Sugiyasu, S. Manna, S. Samitsu and M. Takeuchi, *Nat. Chem.*, 2014, **6**, 188-195.
59 S. H. Jung, D. Bochicchio, G. M. Pavan, M. Takeuchi and K. Sugiyasu, *J. Am. Chem. Soc.*, 2018, **140**, 10570-10577.
60 N. Sasaki, J. Kikkawa, Y. Ishii, T. Uchihashi, H. Imamura, M. Takeuchi and K. Sugiyasu, *Nat. Chem.*, 2023, **15**, 922-929.
61 E. B. Fleischer and A. M. Shachter, *Inorg. Chem.*, 1991, **30**, 3763-3769.
62 D. A. Roberts, T. W. Schmidt, M. J. Crossley and S. Perrier, *Chem. Eur. J.*, 2013, **19**, 12759-12770.
63 K. Ogawa and Y. Kobuke, *Angew. Chem. Int. Ed.*, 2000, **39**, 4070-4073.
64 U. Michelsen and C. A. Hunter, *Angew. Chem. Int. Ed.*, 2000, **39**, 764-767.
65 M. Koepf, J. Conradt, J. Szmytkowski, J. A. Wytko, L. Allouche, H. Kalt, T. S. Balaban and J. Weiss, *Inorg. Chem.*, 2011, **50**, 6073-6082.
66 M. Morisue, Y. Hoshino, M. Shimizu, T. Nakanishi, Y. Hasegawa, M. A. Hossain, S. Sakurai, S. Sasaki, S. Uemura and J. Matsui, *Macromolecules*, 2017, **50**, 3186-3192.
67 A. Satake, Y. Suzuki, M. Sugimoto and Y. Kuramochi, *Chem. Eur. J.*, 2020, **26**, 669-684.
68 S.-G. Chen, Y. Yu, X. Zhao, Y. Ma, X.-K. Jiang and Z.-T. Li, *J. Am. Chem. Soc.*, 2011, **133**, 11124-11127.

ChemComm

View Article Online
DOI: 10.1039/D6CC02170K

Feature Article

69 H. Lee, Y. H. Jeong, J. H. Kim, I. Kim, E. Lee and W. D. Jang, *J. Am. Chem. Soc.*, 2015, **137**, 12394-12399.
70 H. S. W. Lee, H. Park, D. Ryu and W. D. Jang, *Chem. Soc. Rev.*, 2023, **52**, 1947-1974.
71 P. Even and B. Boitrel, *Coord. Chem. Rev.*, 2006, **250**, 519-541.
72 V. Valderrey, G. Aragay and P. Ballester, *Coord. Chem. Rev.*, 2014, **258**, 137-156.
73 C. García-Simón, M. Costas and X. Ribas, *Chem. Soc. Rev.*, 2016, **45**, 40-62.
74 H. Lu and N. Kobayashi, *Chem. Rev.*, 2016, **116**, 6184-6261.
75 J. M. Park, K. I. Hong, H. Lee and W. D. Jang, *Acc. Chem. Res.*, 2021, **54**, 2249-2260.
76 S. Maguire, G. Strachan, K. Norvaisa, C. Donohoe, L. C. Gomes-Da-Silva and M. O. Senge, *Chem. Eur. J.*, 2024, **30**, e202401559.
77 V. V. Borovkov, G. A. Hembury and Y. Inoue, *Acc. Chem. Res.*, 2004, **37**, 449-459.
78 I. Beletskaya, V. S. Tyurin, A. Y. Tsivadze, R. Guilard and C. Stern, *Chem. Rev.*, 2009, **109**, 1659-1713.
79 T. Hirao and T. Haino, *J. Porphyr. Phthalocyanines*, 2023, **27**, 966-979.
80 I. Tabushi, S. Kugimiya, M. G. Kinnaird and T. Sasaki, *J. Am. Chem. Soc.*, 1985, **107**, 4192-4199.
81 X. F. Huang, B. H. Rickman, B. Borhan, N. Berova and K. Nakanishi, *J. Am. Chem. Soc.*, 1998, **120**, 6185-6186.
82 X. F. Huang, N. Fujioka, G. Pescitelli, F. E. Koehn, R. T. Williamson, K. Nakanishi and N. Berova, *J. Am. Chem. Soc.*, 2002, **124**, 10320-10335.
83 J. M. Lintuluoto, V. V. Borovkov and Y. Inoue, *J. Am. Chem. Soc.*, 2002, **124**, 13676-13677.
84 D. Chandel, C. Pal, B. Saha, S. A. Ikbal and S. P. Rath, *Dalton Trans.*, 2022, **51**, 14125-14137.
85 T. Ema, N. Ouchi, T. Doi, T. Korenaga and T. Sakai, *Org. Lett.*, 2005, **7**, 3985-3988.
86 G. A. Hembury, V. V. Borovkov and Y. Inoue, *Chem. Rev.*, 2008, **108**, 1-73.
87 L. P. Hernández-Eguía, R. J. Brea, L. Castedo, P. Ballester and J. R. Granja, *Chem. Eur. J.*, 2011, **17**, 1220-1229.
88 T. Haino, T. Fujii and Y. Fukazawa, *Tetrahedron Lett.*, 2005, **46**, 257-260.
89 N. Hisano, T. Hirao and T. Haino, *Chem. Lett.*, 2021, **50**, 1844-1847.
90 T. Haino, T. Fujii and Y. Fukazawa, *J. Org. Chem.*, 2006, **71**, 2572-2580.
91 N. Hisano and T. Haino, *J. Org. Chem.*, 2022, **87**, 4001-4009.
92 P. Ballester, A. Costa, P. M. Deyà, A. Frontera, R. M. Gomila, A. I. Oliva, J. K. M. Sanders and C. A. Hunter, *J. Org. Chem.*, 2005, **70**, 6616-6622.
93 J. Etxebarria, A. Vidal-Ferran and P. Ballester, *Chem. Commun.*, 2008, **44**, 5939-5941.
94 I. C. Pintre, S. Pierrefixe, A. Hamilton, V. Valderrey, C. Bo and P. Ballester, *Inorg. Chem.*, 2012, **51**, 4620-4635.
95 T. Haino, A. Watanabe, T. Hirao and T. Ikeda, *Angew. Chem. Int. Ed.*, 2012, **51**, 1473-1476.
96 F. H. Huang, D. S. Nagvekar, X. C. Zhou and H. W. Gibson, *Macromolecules*, 2007, **40**, 3561-3567.
97 T. Hirao and T. Haino, *Chem. Rec.*, 2026, **26**, e202500281.
98 Y. Cohen, L. Avram and L. Frish, *Angew. Chem. Int. Ed.*, 2005, **44**, 520-554.
99 R. Schmidt, M. Stolte, M. Grüne and F. Würthner, *Macromolecules*, 2011, **44**, 3766-3776.
100 M. E. Cates, *Macromolecules*, 1987, **20**, 2289-2296.
101 H. Jacobson and W. H. Stockmayer, *J. Chem. Phys.*, 1950, **18**, 1600-1606.
102 G. Ercolani, L. Mandolini, P. Mencarelli and S. Roelens, *J. Am. Chem. Soc.*, 1993, **115**, 3901-3908.
103 G. Ercolani, *J. Phys. Chem. B*, 1998, **102**, 5699-5703.
104 V. M. Krishnamurthy, V. Semetey, P. J. Bracher, N. Shen and G. M. Whitesides, *J. Am. Chem. Soc.*, 2007, **129**, 1312-1320.
105 M. M. C. Bastings, T. F. A. de Greef, J. L. J. van Dongen, M. Merkx and E. W. Meijer, *Chem. Sci.*, 2010, **1**, 79-88.
106 T. F. A. De Greef, M. M. J. Smulders, M. Wolffs, A. P. H. J. Schenning, R. P. Sijbesma and E. W. Meijer, *Chem. Rev.*, 2009, **109**, 5687-5754.
107 A. T. ten Cate, H. Kooijman, A. L. Spek, R. P. Sijbesma and E. W. Meijer, *J. Am. Chem. Soc.*, 2004, **126**, 3801-3808.
108 J. Xu, E. A. Fogleman and S. L. Craig, *Macromolecules*, 2004, **37**, 1863-1870.
109 T. F. A. de Greef, G. Ercolani, G. B. W. L. Ligthart, E. W. Meijer and R. P. Sijbesma, *J. Am. Chem. Soc.*, 2008, **130**, 13755-13764.
110 T. F. E. Paffen, G. Ercolani, T. F. A. de Greef and E. W. Meijer, *J. Am. Chem. Soc.*, 2015, **137**, 1501-1509.
111 M. Ciaccia, I. Tosi, L. Baldini, R. Cacciapaglia, L. Mandolini, S. Di Stefano and C. A. Hunter, *Chem. Sci.*, 2015, **6**, 144-151.
112 S. Di Stefano and G. Ercolani, *J. Phys. Chem. B*, 2017, **121**, 649-656.
113 R. Hu, L. Gao, C. H. Cai, J. P. Lin, Z. W. Chen and L. Q. Wang, *Macromolecules*, 2021, **54**, 5196-5203.
114 T. Hirao, N. Hisano, S. Akine, S. Kihara and T. Haino, *Macromolecules*, 2019, **52**, 6160-6168.
115 T. F. A. Greef and E. W. Meijer, *Nature*, 2008, **453**, 171-173.
116 T. Aida, E. W. Meijer and S. I. Stupp, *Science*, 2012, **335**, 813-817.
117 A. Harada, A. Hashidzume, H. Yamaguchi and Y. Takashima, *Chem. Rev.*, 2009, **109**, 5974-6023.
118 L. L. Yang, X. X. Tan, Z. Q. Wang and X. Zhang, *Chem. Rev.*, 2015, **115**, 7196-7239.
119 L. Voorhaar and R. Hoogenboom, *Chem. Soc. Rev.*, 2016, **45**, 4013-4031.
120 M. Häring and D. D. Díaz, *Chem. Commun.*, 2016, **52**, 13068-13081.
121 T. Haino, *Polym. J.*, 2019, **51**, 303-318.
122 P. K. Hashim, J. Bergueiro, E. W. Meijer and T. Aida, *Prog. Polym. Sci.*, 2020, **105**, 101250.
123 T. D. Clemons and S. I. Stupp, *Prog. Polym. Sci.*, 2020, **111**, 101310.
124 S. Datta, S. Takahashi and S. Yagai, *Acc. Mater. Res.*, 2022, **3**, 259-271.
125 G. Sinawang, M. Osaki, Y. Takashima, H. Yamaguchi and A. Harada, *Chem. Commun.*, 2020, **56**, 4381-4395.
126 H. Lee, J. Kim, M. Lee and J. Kang, *Chem. Rev.*, 2025, **125**, 11379-11425.
127 N. Hisano, T. Hirao and T. Haino, *Chem. Commun.*, 2020, **56**, 7553-7556.
128 T. Ikeda, A. Watanabe, T. Oshita and T. Haino, *Heteroatom Chem.*, 2011, **22**, 590-593.
129 S. E. Towell, M. J. Jareczek, L. S. Cooke, D. R. Godfrey and A. V. Zhukhovitskiy, *Acc. Chem. Res.*, 2025, **58**, 1275-1283.
130 Y. X. Zhang, D. Yang, X. Li, P. A. Chen, X. K. Yao and Z. B. Jian, *Natl. Sci. Rev.*, 2025, **12**, nwaf489.
131 R. A. J. Ditzler, A. J. King, S. E. Towell, M. Ratushnyy and A. V. Zhukhovitskiy, *Nat. Rev. Chem.*, 2023, **7**, 600-615.

ChemComm

View Article Online
DOI: 10.1039/D6CC02170K

Feature Article

132 T. Haino, T. Fujii, A. Watanabe and U. Takayanagi, *Proc. Natl. Acad. Sci. USA*, 2009, **106**, 10477-10481.
133 K. Nadamoto, K. Maruyama, N. Fujii, T. Ikeda, S.-i. Kihara and T. Haino, *Angew. Chem. Int. Ed.*, 2018, **57**, 7028-7033.
134 E. Yashima and K. Maeda, *Bull. Chem. Soc. Jpn.*, 2021, **94**, 2637-2661.
135 B. P. Bloom, Y. Paltiel, R. Naaman and D. H. Waldeck, *Chem. Rev.*, 2024, **124**, 1950-1991.
136 E. Yashima, N. Ousaka, D. Taura, K. Shimomura, T. Ikai and K. Maeda, *Chem. Rev.*, 2016, **116**, 13752-13990.
137 R. T. Gao, S. Y. Li, N. Liu, B. H. Liu and Z. Q. Wu, *Chem. Rev.*, 2026, **126**, 297-403.
138 Y. C. Guo, Y. F. Zhang, J. F. Ma, R. Liao and F. Wang, *Nat. Commun.*, 2024, **15**, 9303.
139 R. Chen, A. Hammoud, P. Aoun, M. A. Martínez-Aguirre, N. Vanthuyne, R. Maruchenko, P. Brocorens, L. Bouteiller and M. Raynal, *Nat. Commun.*, 2024, **15**, 4116.
140 F. Helmich, C. C. Lee, A. P. H. J. Schenning and E. W. Meijer, *J. Am. Chem. Soc.*, 2010, **132**, 16753-16755.
141 R. Abbel, C. Grenier, M. J. Pouderoijen, J. W. Stouwdam, P. E. L. G. Leclère, R. P. Sijbesma, E. W. Meijer and A. P. H. J. Schenning, *J. Am. Chem. Soc.*, 2009, **131**, 833-843.
142 N. Hisano, T. Kodama, S. Koya and T. Haino, *Chem. Eur. J.*, 2025, **31**, e202404210.
143 N. Fujii, N. Hisano, T. Hirao, S.-I. Kihara, K. Tanabe, M. Yoshida, S.-I. Tate and T. Haino, *Angew. Chem. Int. Ed.*, 2025, **64**, e202416770.
144 K. Maeda, D. Hirose, M. Nozaki, Y. Shimizu, T. Mori, K. Yamanaka, K. Ogino, T. Nishimura, T. Taniguchi, M. Moro and E. Yashima, *Sci. Adv.*, 2021, **7**, eabg5381.
145 M. Quan, X. Y. Pang and W. Jiang, *Angew. Chem. Int. Ed.*, 2022, **61**, e202201258.
146 K. Kato, S. Fa and T. Ogoshi, *Angew. Chem. Int. Ed.*, 2023, **62**, e202308316.
147 H. Zhu, Q. Li, Z. Gao, H. Wang, B. Shi, Y. Wu, L. Shangguan, X. Hong, F. Wang and F. Huang, *Angew. Chem. Int. Ed.*, 2020, **59**, 10868-10872.
148 T. Hirao, S. Kishino and T. Haino, *Chem. Commun.*, 2023, **59**, 2421-2424.
149 T. Hirao, S. Kishino, M. Yoshida and T. Haino, *Chem. Eur. J.*, 2024, **30**, e202403569
150 K. Kinjo, T. Hirao, S.-i. Kihara, Y. Katsumoto and T. Haino, *Angew. Chem. Int. Ed.*, 2015, **54**, 14830–14834.
151 R. P. Sijbesma, F. H. Beijer, L. Brunsveld, B. J. B. Folmer, J. H. K. K. Hirschberg, R. F. M. Lange, J. K. L. Lowe and E. W. Meijer, *Science*, 1997, **278**, 1601-1604.
152 R. K. Castellano, R. Clark, S. L. Craig, C. Nuckolls and J. Rebek, Jr., *Proc. Natl. Acad. Sci. USA*, 2000, **97**, 12418-12421.
153 D. W. R. Balkenende, C. A. Monnier, G. L. Fiore and C. Weder, *Nat. Commun.*, 2016, **7**, 10995.

Author bibliography

Takeharu Haino received his doctoral degree from Hiroshima University in 1992 after which he joined the Sagami Chemical Research Center. In 1993, he became an assistant professor at Hiroshima University. In 1999, he was a visiting researcher with Professor Rebek's team at The Scripps Research Institute. He was promoted to associate professor in 2000, attained the status of full professor in 2007, and was recognized as a distinguished professor in 2021. In addition, he serves as an associate editor for the Bulletin of the Chemical Society of Japan.

Takehiro Hirao earned his Ph.D. in Chemistry from Hiroshima University in 2016. He served as a postdoctoral researcher in Professor Sessler's group at the University of Texas at Austin. In 2018, he became an assistant professor at Hiroshima University and is currently an associate professor. His research focuses on designing and developing structurally well-defined supramolecular complexes.

Naoyuki Hisano obtained his Ph.D. in Chemistry from Hiroshima University in 2022. He then conducted postdoctoral research with Professor Pablo Ballester at the Institut Català d'Investigació Química (ICIQ). In 2023, he became an assistant professor at Hiroshima University. His research focuses on the design and development of supramolecular complexes and structures.

View Article Online
DOI: 10.1039/D6CC02170K

No new data were created in the course of preparing this manuscript. All the data sources mentioned in the article are publicly accessible and have been properly cited.